Research Paper

PAIN

VIDEO

A transcriptional toolbox for exploring peripheral neuroimmune interactions

Zhi Liang, Zoe Hore, Peter Harley, Federico Uchenna Stanley, Aleksandra Michrowska, Monica Dahiya, Federica La Russa, Sara E. Jager, Sara Villa-Hernandez, Franziska Denk*

Abstract

Correct communication between immune cells and peripheral neurons is crucial for the protection of our bodies. Its breakdown is observed in many common, often painful conditions, including arthritis, neuropathies, and inflammatory bowel or bladder disease. Here, we have characterised the immune response in a mouse model of neuropathic pain using flow cytometry and cell-type-specific RNA sequencing (RNA-seq). We found few striking sex differences, but a very persistent inflammatory response, with increased numbers of monocytes and macrophages up to 3 1/2 months after the initial injury. This raises the question of whether the commonly used categorisation of pain into "inflammatory" and "neuropathic" is one that is mechanistically appropriate. Finally, we collated our data with other published RNA-seq data sets on neurons, macrophages, and Schwann cells in naive and nerve injury states. The result is a practical web-based tool for the transcriptional data mining of peripheral neuroimmune interactions. http://rna-seq-browser.herokuapp.com/

Keywords: Peripheral neuroimmune interactions, RNA-seq, Myeloid cells, Neuropathic pain, Inflammatory pain

1. Introduction

The immune and peripheral nervous systems are closely entwined. A complex network of sensory and sympathetic fibres innervates our organs and engages in bidirectional communication with a host of tissue resident immune cells, including macrophages, dendritic cells, and T lymphocytes. A disruption in this neuroimmune connection contributes to many common debilitating conditions, including chronic pain, which is estimated to affect nearly 1 in 5 people in the general European population.[9] Pain in its acute form is a natural consequence and cardinal sign of inflammation.[44] By contrast, chronic pain can become uncoupled from underlying disease, causing independent nervous system dysfunction, which requires bespoke treatment approaches. In recognition of this, chronic pain syndromes have just been added to the World Health Organization's *International Classification of Diseases* (*ICD-11*).[63]

A primary driver for the uncoupling between pain and acute inflammation is believed to be release of proalgesic mediators from nonneuronal cell types. This process, known as peripheral sensitisation, causes sensory neurons to become spontaneously active and hypersensitive to normally innocuous stimuli.[37,45,53] Many different cell types have been implicated in peripheral sensitisation, including immune cells, satellite glial cells, and Schwann cells.[4,14,55] Already 2 decades ago, for example, both neutrophils and macrophages were reported to be causally involved in hyperalgesia—an exaggerated pain sensation in response to a noxious stimulus.[42,47] Nevertheless, the details of this connection remain vague, with agreement in the preclinical literature largely limited to the one main finding that interfering with various subtypes of myeloid cell will alter evoked pain behaviour in various animal models of persistent pain.[5,16,31,46] Mechanistically, this has been ascribed to different mediators putatively released from macrophages and neutrophils, chiefly among them tumor necrosis factor, interleukin 1 beta, interleukin 6, and nerve growth factor.[4,36,55]

The current lack of precision is hardly surprising when we consider the incredible cellular and functional complexity of our bodies' inflammatory process.[1] Each tissue mounts its own distinct local inflammatory responses that, at their peak, are usually accompanied by systemic endocrine effects resulting in diverse symptoms including fever and fatigue. The correct interplay of these responses is essential for efficient immunity and tissue healing, as is a very tightly controlled resolution process—which again relies on several active, parallel intercellular and intracellular mechanisms.[2,43]

Here, we aim to provide a more detailed view of immune cell responses in a persistent pain state. We used partial sciatic nerve ligation (PSNL) as a model of traumatic neuropathic pain and performed flow cytometry analysis and fluorescence-activated cell sorting on male and female mice over a 3 1/2-month time course. RNA-seq was performed at 1 and 10 weeks after nerve injury on immune cell subpopulations (**Fig. 1A**) extracted from sciatic nerve and the ganglia in which its cell bodies are located: lumbar L3-L5 dorsal root ganglia (DRG). Our results were integrated with other publicly available data of relevant cell types

Sponsorships or competing interests that may be relevant to content are disclosed at the end of this article.

Z. Liang and Z. Hore contributed equally to this work.

Wolfson Centre for Age-Related Diseases, Institute of Psychiatry, Psychology and Neuroscience, King's College London, Guy's Campus, London, United Kingdom

**Corresponding author. Address: Wolfson Centre for Age-Related Diseases, Institute of Psychiatry, Psychology and Neuroscience, King's College London, Guy's Campus, London SE1 1UL, United Kingdom. Tel.: 0044 207 848 8054. E-mail address: franziska.denk@kcl.ac.uk (F. Denk).*

Supplemental digital content is available for this article. Direct URL citations appear in the printed text and are provided in the HTML and PDF versions of this article on the journal's Web site (www.painjournalonline.com).

PAIN 161 (2020) 2089–2106

http://dx.doi.org/10.1097/j.pain.0000000000001914

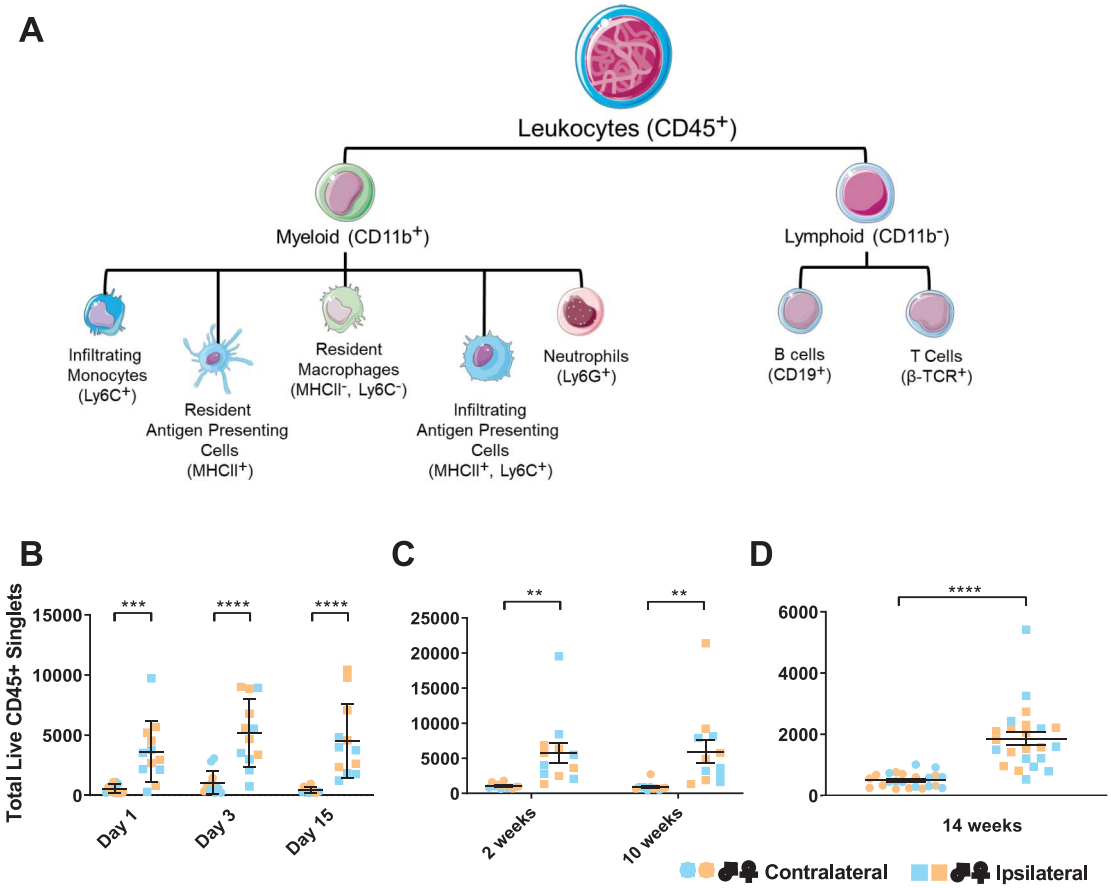

Figure 1. Partial sciatic nerve ligation induces a long-lasting increase in total CD45$^+$ immune cell counts in sciatic nerve. (A) Schematic of the markers used to differentiate lymphoid and myeloid immune cell populations in flow cytometry and FACS experiments. (B–D) Plotted are the total number of live CD45+ singlets isolated from sciatic nerve after partial sciatic nerve ligation at different time points. Results were obtained as part of 3 separate experimental batches (B–D). In (B) and (C), n = 12 mice per time point (6 males in blue and 6 females in orange) were processed, whereas in (D), n = 23 mice (11 males & 12 females) were processed, shown here as separate data points with mean ± SEM.

to generate a plug-and-play, user-friendly website for interrogating peripheral neuroimmune interactions at transcriptional level.

2. Methods

2.1. Animals

Male and female C57BL/6 J mice were purchased from Envigo Ltd, London, United Kingdom at 5 to 6 weeks of age and acclimatised to the animal unit for one week before surgeries. They were housed in standard individually ventilated cages (Tecniplast, London, United Kingdom) in groups of 5 maximum at a 12-hour light–dark cycle, with ad lib access to food and water. All experiments described were conducted in accordance with the United Kingdom Home Office Legislation (Scientific Procedures Act, 1986) and were approved by the Home Office to be conducted at King's College London under project license number P57A189DF. None of our experiments required pooling of animals, so n refers to tissue or cells obtained from individual mice.

2.2. Surgeries

Mice underwent PSNL surgery, using a paradigm originally developed in the rat.[56] Briefly, animals were anesthetised under isoflurane (Henry Schein, Melville, NY, Cat# 988-3245) and administered 0.05 mg/kg of the analgesic buprenorphine subcutaneously. After shaving the fur covering the left hip and leg region, the sciatic nerve was exposed through blunt dissection and roughly half was tightly ligated with a 5.0 suture (Ethicon, Cincinnati, OH, Cat# W9982). The wound was stapled shut, and mice were transferred to a clean cage and left to recover in the animal unit. Animals were weighed and monitored regularly (at least triweekly) after surgery.

2.3. Processing of sciatic nerve and dorsal root ganglia

Mice were administered an intraperitoneal overdose of pentobarbital (Euthatal; Merial, Duluth, GA, Lot# P02601A) and perfused with 10 mL of 1 × phosphate buffered saline (PBS) to avoid peripheral blood contamination. The ligated sciatic nerve was exposed (Supplementary Figure 1, available at http://links.lww.com/PAIN/B19) and followed up towards the spinal cord to identify and dissect out L3-L5 DRG into F12 (Gibco, New York, NY, Cat# 21765-029). The nerve itself was also placed into a Petri dish containing F12 and cut to 0.5 cm, ensuring equal lengths of nerve either side of the ligature. If still present, the ligature itself was removed with tweezers. This process was repeated for the uninjured contralateral side, with pains being taken to ensure harvesting from a similar segment of nerve (again 0.5 cm in length). Tissues were kept in F12 on ice until all animals in a given batch were processed and then transferred into wells of a standard polymerase chain reaction (PCR) plate (Starlab, Milton Keynes, United Kingdom, Cat # E1403-0100) containing 50 μL of

digestion mix: F12 with 6.25 mg/mL collagenase type IA (Sigma Aldrich, Poole, United Kingdom, Cat# C9891), 0.4% wt/vol hyaluronidase (ABNOVA, Slough, United Kingdom, Cat# P52330), and 0.2% wt/vol pronase (Millipore, Watford, United Kingdom, Cat# 53702) for nerve; F12 with 3 mg/mL dispase II (Sigma Aldrich, Cat# 04942078001), 12.5 mg/mL collagenase type IA (Sigma Aldrich, Cat# C9891), and 10 mg/mL DNase I (Sigma Aldrich, Cat# 10104159001) for DRG. For optimal digestion, nerves were chopped into small pieces with spring scissors (50x chops, cleaning scissors with 100% ethanol between samples) and incubated at 37˚C, shaking at 220 RPM for 30 minutes. The digestion mix was subsequently removed and replaced with 100 μL of fluorescence-activated cell sorting (FACS) buffer: Hank's balanced salt solution (HBSS) (Gibco, Cat# 14175095) with 0.4% bovine serum albumin (Sigma-Aldrich, Cat# A3983), 15 mM HEPES (Gibco, New York, NY, USA, Cat# 15630080), and 2 mM EDTA (Invitrogen, Waltham, MA, Cat# 15575-038). Samples were dissociated by pipetting up and down 50x and passed through 70-μm Flowmi cell strainers (SP Scienceware, Warminster, PA, Cat# 136800070) into a 96-well v-bottom plate. The plate was centrifuged at 1500 RPM for 5 minutes at 4˚C, supernatant was removed, and the pellets then underwent antibody staining as described in the following.

2.4. Flow cytometry/FACS

On ice, cells were incubated in fixable viability dye in HBSS for 15 minutes, followed by 15-minute incubation in a mix of directly conjugated antibodies and fragment crystallizable (Fc) block (see Supplementary Table 1 for antibody panels and concentrations, available at http://links.lww.com/PAIN/B19). After staining, cells were centrifuged for 5 minutes (1500 RPM at 4˚C) and supernatant was removed. For flow cytometry experiments only, pellets were fixed in 4% paraformaldehyde (PFA) for 5 minutes, the plate was then centrifuged for 5 minutes (1500 RPM at 4˚C), and supernatant was discarded. Finally, pellets were resuspended in 200 μL of FACS buffer. Flow cytometry and FACS were performed at the NIHR BRC flow core facility at King's College London on a BD Fortessa and BD FACSAria, respectively. Unstained cells and single staining control beads (BD Bioscience, Franklin Lakes, NJ, Cat# 552845 for antibodies; Invitrogen, Cat# A10346 for the viability dye) were used for compensation. Fluorescence-minus one controls were recorded and used for gating (see Supplementary Figures 2 and 3 for gating strategies used, available at http://links.lww.com/PAIN/B19). For FACS experiments, 20 cells were collected per population of interest. This choice in number was driven by the temporal constraints of the sort and the technical constraints of the Smart-seq2 cell lysis buffer. It means that our results are more variable compared to traditional bulk sequencing experiments. Analyses were conducted using FlowJo software.

2.5. RNA sequencing

RNA from FACS collected samples was reverse transcribed into cDNA, amplified, and purified in accordance with the Smart-seq2 method.[48] Samples were then run on a High-Sensitivity DNA chip (Agilent, Santa Clara, CA, Cat# 5067-4626) on a 2100 Bioanalyzer (Agilent, Cat# G2939BA) to determine quality and concentration. SMARTer amplified cDNA was shipped to the Oxford Genomics Centre for batch-controlled library preparation using an Illumina NexteraXT kit (Illumina, San Diego, CA, Cat# FC-131-1096) and sequenced on an Illumina HiSeq 4000 (75 bp, paired-end reads).

2.6. RNA-seq data analysis

Basic quality control was conducted in seqmonk on stampy bam files[35] obtained from the sequencing facility. For detailed analysis, fastq files were trimmed by Trimmomatic[7] (version-0.39) to eliminate reads with phred scores less than 33 and remove any residual adapters. The reads were then pseudoaligned using kallisto[8] (version 0.46.0) with the following command parameters: *kallisto quant -i transcripts.idx -o output -b 100 [lane1].fastq [lane2].fastq [lane3].fastq*. The *transcripts.idx* file was built from Ensembl v96 transcriptomes according to instructions provided by the Pachter Lab (https://github.com/pachterlab/kallisto-transcriptome-indices/releases). Raw transcript counts were length and depth corrected by conversion to transcripts per million (TPM) using the R package tximport[58] and the transcripts_to_genes file provided on the kallisto website. The R package sleuth[49] was used for differential expression analysis (Wald test for 2-group comparisons, likelihood ratio test for multiple group comparisons). Power simulations were conducted using the R package powsimR.[67] Data were deposited in the Gene Expression Omnibus (GEO) archive, accession number GSE139150.

To generate our web-tool, we also ran our data through kallisto on BioJupies[62] to be able to compare our results to those of other published cell-type-specific data sets in the same format. BioJupies is a reanalysis tool based on ARCHS4[29]—a project with one common kallisto pipeline to realign all human and mouse RNA-seq experiments that were run on HiSeq 2000, HiSeq 2500, and NextSeq 500 platforms and deposited on either GEO or the Short Read Archive. We accessed cell types analysed in their naive state, in regeneration models (sciatic nerve transection and crush) and in persistent pain models (sciatic nerve ligation). In particular, we compiled: magnetically sorted sensory neurons and FAC-sorted satellite glia before and after nerve ligation (GSE120284),[24] Schwann cells sorted after sciatic nerve transection (GSE103039),[10] macrophages after sciatic nerve transection (GSE106488),[61] CCR2+Cx3cr1+ macrophages after sciatic nerve crush (GSE106927),[59] and naive macrophages associated with sympathetic nerve and ganglia in adipose tissue (GSE103847).[50]

2.7. Behavioural assay

Behavioural data were collected at ~13.5 weeks after PSNL. Because mice with PSNL display paw guarding, we reasoned that it would not be feasible to maintain blinding during conventional von Frey behavioural testing. We therefore designed a new simple paradigm to score the visible discomfort in mice in a blinded fashion. Behaviours were video-taped and later scored by 2 individuals unfamiliar with pain models and our hypothesis, and who were unable to distinguish between male and female mice. For the test, mice were left to freely explore an open arena of 20 cm in diameter—once for 5 minutes 2 days before testing without video recording for acclimatisation and once for 2 minutes with video recording. Videos were scored for deficits to the ipsilateral and contralateral legs and hind paws using a simple 0 to 2 scale, whereby 0 = no deficit, 1 = slight paw clenching, and 2 = severe paw clenching and/or dragging of leg. Numbers were awarded every 30 seconds so that each mouse received a total deficit score out of 8. Scoring was performed on each hind leg separately. Final scores were aggregated through averaging of the individual scores obtained by the 2 independent observers.

2.8. Immunohistochemistry

At 14 weeks after PSNL surgery, mice were overdosed with pentobarbital and perfused with 10 mL of 1 × PBS, followed by 20

mL of 4% PFA. 0.5 cm of ipsilateral and contralateral sciatic nerves were dissected as described above for flow cytometry. Nerves were then postfixed in 4% PFA for 2 hours, washed in 1 × PBS, and cryoprotected in 30% sucrose. After this, nerves were embedded in optimal cutting temperature compound (OCT) (CellPath, Newtown, United Kingdom, KMA-0100-00A) and cut sagittally into 20-μm sections on a cryostat. For immunofluorescent staining, sections were incubated for 4 hours in blocking serum (10% donkey serum, 0.2% triton in PBS) and stained overnight with primary antibodies against IBA1 (rabbit, 1:500, Wako, Osaka, Japan, 019-19741), CD68 (mouse, 1:500, Abcam, Cambridge, United Kingdom, ab31630), and directly conjugated MHCII (1:500, BioLegend, San Diego, CA, 107607). After 3 washes in PBS, sections were incubated with secondary antibodies for 2 hours—Alexa Fluor 647 (goat anti-rabbit, 1:1000, Invitrogen, A21244) and Alexa Fluor 568 (donkey anti-mouse, 1:1000, Invitrogen, A10037). After 3 further washes in PBS, sections were mounted using Fluoromount-G mounting medium with DAPI (Invitrogen, 00-4959-52) and imaged on a Zeiss LSM 710 confocal microscope.

2.9. Bone marrow-derived macrophage culture and quantitative reverse transcription PCR (qRT-PCR)

Bone marrow-derived macrophages were isolated from C57BL/6 J mice and cultured in Petri dishes containing Dulbecco's Modified Eagle's Medium (DMEM) (Gibco, 32430-027) supplemented with 10% (vol/vol) fetal bovine serum (10500-064) and Pen/Strep (Sigma Aldrich, P4333). Femur and tibia bones from both hind limbs of female mice were collected and the bone marrow was flushed out with cold PBS (Gibco, 14190-094) under sterile conditions using a 10-mL syringe with a 25G needle. Cells were centrifuged (7 minutes, 2000 rpm, room temperature) and the pellet was resuspended in DMEM with macrophage colony stimulating factor (DMEM-MCSF) (Peprotech, London, United Kingdom, 315-02). The suspension was passed through a 40-μm cell strainer to filter out bone fragments. Flow-through was collected and filled up to 50 mL with prewarmed DMEM-MCSF. The cell suspension was plated onto two 15-cm Petri dishes (25 mL/dish) and incubated (37°C, 5% CO_2) for 7 days to allow for differentiation into mature naive macrophages. After 7 days of incubation, the culture supernatants were discarded and the remaining adherent cells were washed with 15 mL of prewarmed PBS. Cells were incubated (37°C, 5% CO_2) with 15 mL of prewarmed nonenzymatic cell dissociation solution (Sigma Aldrich, CAT#S-014-B) for 10 minutes and then gently dislodged with a cell scraper and centrifuged for collection (7 minutes, 1800 rpm, room temperature). The cells were plated at 5×10^5/well in 12 multiwell plates or 24 multiwell plates and left to settle overnight in DMEM (w/o MCSF). The next day, cells were incubated for 24 hours in: interferon gamma, IFNγ, 50 ng/mL (PeproTech, 315-05) or lipopolysaccharide, LPS, 100 ng/mL (Sigma, L4391) or interleukin 4, IL-4, 50 ng/mL (Miltenyi Biotec, Bergisch Gladbach, Germany, 130-097-760), either alone or in combination with calcitonin gene-related peptide, CGRP, 100 ng/mL (Bachem, Bubendorf, Switzerland, H-1470). Unstimulated cells were incubated in plain DMEM as a control. For RNA extraction, bone marrow-derived macrophages were lysed (RLT-buffer+ β-mercaptoethanol) and RNA was extracted using the RNAeasy Microkit 50 (Qiagen, Hilden, Germany, 74004) according to manufacturer's instructions. mRNA quantity was evaluated using Qubit 3 Fluorometer (Invitrogen) or Bioanalyzer (Agilent RNA pico chip). 124 to 1548 ng of RNA was converted into cDNA using SuperScript III Reverse Transcriptase (Invitrogen, 18080-044) according to manufacturer's instructions. 6.2 ng/μL of cDNA was used in standard SYBR Green (Roche, Basel, Switzerland, 39355320) qRT-PCR reactions on a LightCycler 480 (Roche) to quantify expression of proenkephalin, *Penk* (forward GAGAG-CACCAACAATGACGAA; reverse TCTTCTGGTAGTCCATC-CACC). The geometric mean of the housekeeping gene 18s was used to calculate $2^{-\Delta Ct}$ values.

2.10. qRT-PCR validation of sequencing data

The below primer sequences were used to assess the expression level of *Apoe, Trem2,* and *Tmem119* in additional biological replicates of MHCII+ nerve/DRG macrophages and MHCII-/Ly6C- DRG macrophages. All primers, including the Penk primer above, were tested for their efficiency and specificity.

2.11. Statistical analysis

Cell counts were analysed in GraphPad Prism using either Student *t*-tests, or two-way ANOVAs with *time* and *injury* as independent variables, followed by Sidak post hoc tests (**Figs. 1–6**). qRT-PCR of *Penk* expression was analysed using a nonparametric Kruskal–Wallis ANOVA followed by Dunn post hoc tests. The behavioural test in Supplementary Figure 4 was analysed in GraphPad Prism using a two-way ANOVA followed by Sidak post hoc tests, available at http://links.lww.com/PAIN/B19. The qRT-PCR data in the Supplementary Materials were analysed using two-way ANOVAs with either *tissue* and *injury* or *sex* and *injury* as main effects, available at http://links.lww.com/PAIN/B19.

3. Results

3.1. Persistent changes in immune cell numbers in nerve after partial sciatic nerve ligation

To develop a detailed characterisation of immune responses in the mouse sciatic nerve after PSNL, we performed 3 batches of flow cytometry experiments at different time points. In each instance, we used a minimum of 6 male and 6 female mice. In every experiment, the total number of live $CD45^+$ immune cells was significantly elevated in ipsilateral nerves compared to their contralateral counterparts (**Figs. 1B–D**, and see Supplementary Figure 5 for a comparison to sham surgery at day 1, available at http://links.lww.com/PAIN/B19). For instance, 14 weeks (3 1/2 months) after PSNL, there were on average 3.7× more immune cells in ipsilateral nerve, a highly statistically significant result (Welch independent-samples *t* test, $t(24) = 6.13$, $P < 0.0001$). A direct, batch-controlled comparison of

Gene	Forward primer sequence	Reverse primer sequence	Product size
Ywhaz	GAAAAGTTCTTGATCCCCAATGC	TGTGACTGGTCCACAATTCCTT	134
Apoe	GACCCAGCAAATACGCCTG	CATGTCTTCCACTATTGGCTCG	79
Trem2	TTGCTGGAACCGTCACCATC	ACTTGGGCACCCTCGAAAC	199
Tmem119	CCTACTCTGTGTCACTCCCG	CACGTACTGCCGGAAGAAATC	212

immune cells collected 2 and 10 weeks (2 1/2 months) after PSNL showed that there was no major difference in immune cell numbers at these 2 points, with a two-way ANOVA revealing no significant main effect ($F(1,44) = 0.01$, $P = 0.96$) or interaction with time ($F(1,44) = 0.03$, $P = 0.87$). The effect of injury on cell number was once more highly significant: $F(1,44) = 20.93$, $P < 0.0001$. Moreover, using immunofluorescence, high numbers of immune cells were still clearly visible 14 weeks after PSNL (Supplementary Figure 6, available at http://links.lww.com/PAIN/B19).

This is quite striking, given that, macroscopically, the site of injury is drastically different weeks vs months after ligation (Supplementary Figure 1, available at http://links.lww.com/PAIN/B19): 2 to 3 months after surgery, any visible signs of the suture have completely disappeared, with only slight swelling and discoloration remaining on the ipsilateral side. Nevertheless, mice still display overt pain-like behaviours at 3 1/2 months, with paws being visibly clenched and/or placed gingerly on any surface (Supplementary Figure 4, available at http://links.lww.com/PAIN/B19). We did not conduct testing over time, and therefore were

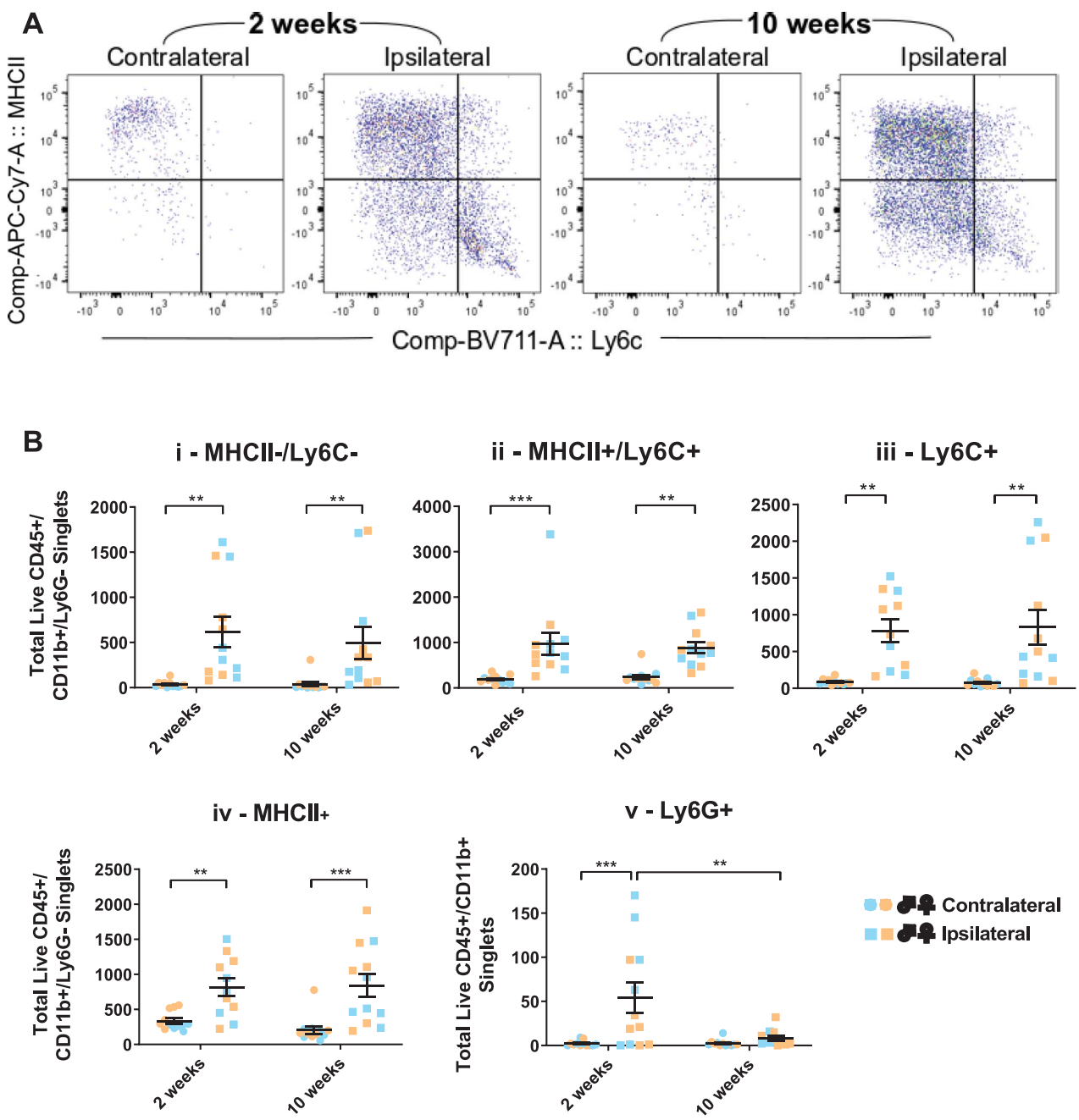

Figure 2. All major myeloid cell populations apart from neutrophils are still upregulated in sciatic nerve two and a half months after partial nerve ligation. (A) Flow cytometry was used to phenotype the major myeloid cell populations in sciatic nerve. Shown here are representative dot plots of 4 of the 5 major myeloid subpopulations, gated on live CD45+, CD11b+, Ly6G- singlets: MHCII+ (likely resident, antigen presenting macrophages), MHCII+/Ly6C+ (likely infiltrating monocytes differentiating into resident populations), Ly6C+ (infiltrating monocytes), and MHCII−/Ly6C− (likely resident macrophages). Note the presence of the MHCII+/Ly6C+ double-positive population and infiltrating Ly6C+ monocytes (hi and lo) primarily after nerve injury. (B) Quantification of the total number of live CD45+/CD11b+ singlets obtained from ipsilateral and contralateral nerves that were either negative for (i) MHCII−/Ly6C− or positive for (ii) MHCII+/Ly6C+, (iii) Ly6C+, (iv) MHCII+, or (v) Ly6G+ (neutrophils). At each time point, n = 12 mice were processed (6 males in blue and 6 females in orange), shown here as separate data points with mean ± SEM.

not in a position to correlate the extent of inflammation with these behaviours.

Detailed flow cytometry analysis revealed that the persistent increase in CD45$^+$ cells is due to an increase in all immune cell types present in nerve, with the exception of Ly6G+ neutrophils (**Fig. 2**; and Supplementary Figure 7, available at http://links.lww.com/PAIN/B19). We observed MHCII+ single positive myeloid cells and MHCII−/LyC6− double-negative myeloid cells in contralateral nerves. After nerve injury, 2 additional populations appeared: Ly6C+ single-positive and MHCII+/Ly6C+ double-positive cells (see Supplementary Figures 2 and 3 for gating strategies, and Supplementary Table 1 for panels, available at http://links.lww.com/PAIN/B19). All 4 populations were significantly upregulated 1 to 3 days, 2, 10, and 14 weeks after injury. Comparing 2 vs 10 weeks, there was no significant main effect of *time* ($F(1,22) = 0.48$, $P = 0.495$) nor an interaction between *time* and *injury* ($F(1,22) = 0.33$, $P = 0.572$).

Similar to CD11b+/Ly6G− populations, αβ+ T cells and CD11b−/Ly6G− populations were also increased on the ipsilateral side (**Fig. 3**; and Supplementary Figure 8, available at http://links.lww.com/PAIN/B19), starting from around 3 days after injury. Absolute event counts remained elevated up to 14 weeks after injury. As we observed previously in DRG,[34] nerve seemed to contain a large population of unidentified CD45$^+$ cells that are nonmyeloid (CD11b−) and not positive for αβ T cell receptor (TCR). They also do not seem to be positive for CD19 (B cells), and preliminary trials indicated that they are negative for γδ+ TCR or glutamine synthetase, a satellite glial cell marker (data not shown). In contrast to the other myeloid populations (CD11b+/Ly6G−), neutrophil numbers (CD11b+/Ly6G+) peaked at day 1 and were still somewhat elevated 2 weeks after PSNL, but then dropped back to contralateral levels (**Fig. 2**; and Supplementary Figure 7, available at http://links.lww.com/PAIN/B19).

3.2. Few striking differences in dorsal root ganglia cell numbers after partial sciatic nerve ligation

The picture emerging from DRG was different (**Figs. 4 and 5**; Supplementary Figure 5, available at http://links.lww.com/PAIN/B19), with the increase in the total number of live CD45$^+$ cells being much less pronounced. Our first batch of experiments collecting cells 1, 3, and 15 days after injury showed no differences in overall immune cell numbers (**Fig. 4A**). In a second batch of experiments (**Figs. 4B and 5**) collecting cells 14 days and 10 weeks after injury, a two-way ANOVA revealed significant main effects of *injury* ($F(1,43) = 13.03$, $P < 0.001$) and *time* ($F(1,43) = 5.44$, $P = 0.024$), with a significant increase in immune cell numbers in ipsilateral DRG only at 2 weeks (adj. $P = 0.003$). The fact that the difference at 14 days was small and not detectable in our first batch of experiments could mean that total CD45$^+$ numbers in DRG are not altered. However, this seems unlikely, given many prior reports of changes in immune cell numbers in DRG in the literature.[26,52,66,72] Instead, we

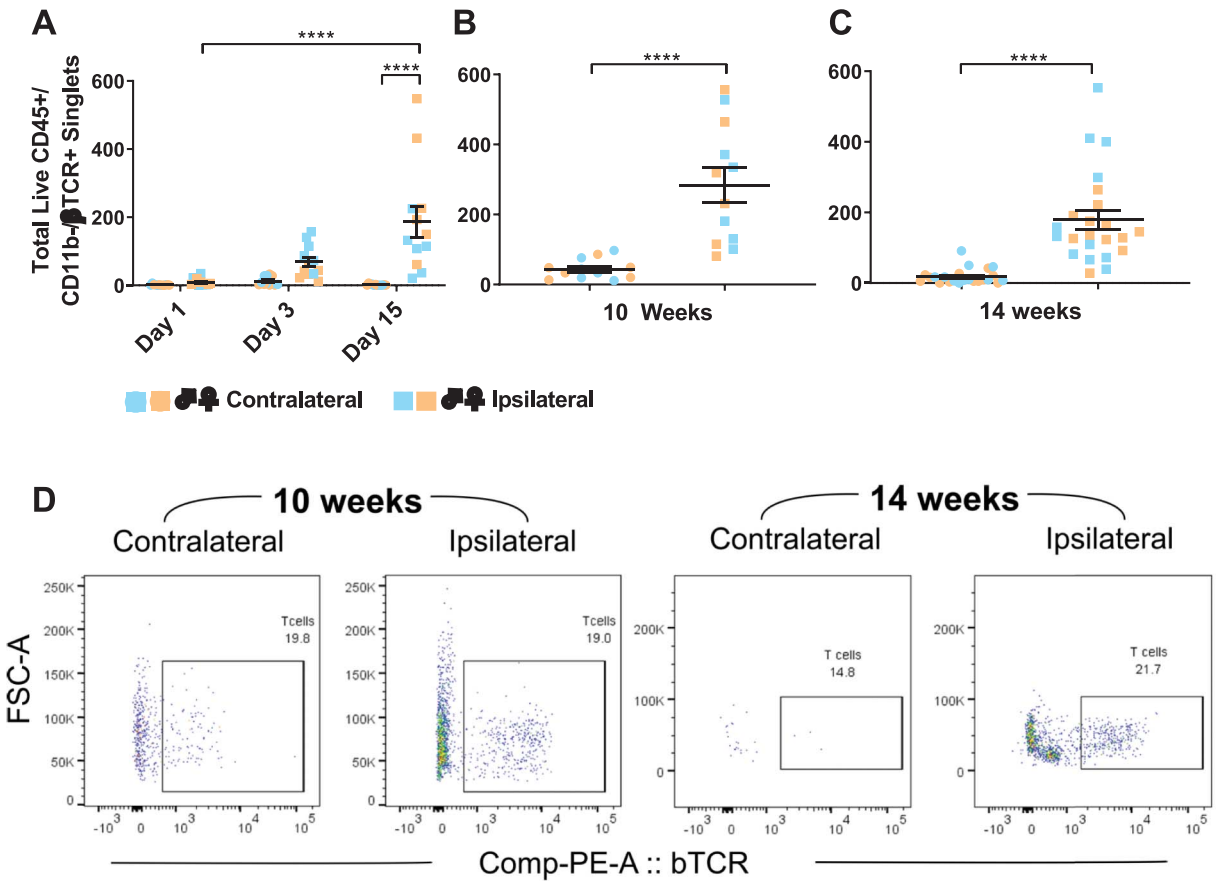

Figure 3. Partial sciatic nerve ligation induces a long-lasting increase in αβ T-cell counts in sciatic nerve. Plotted are the total number of live CD45+/CD11b−/βTCR+ singlets isolated from sciatic nerve after partial sciatic nerve ligation at different time points. Results were obtained as part of 3 separate experimental batches (A–C). In (A) and (B), n = 12 mice per time point (6 males in blue and 6 females in orange) were processed, whereas in (C) n = 23 mice (11 males & 12 females) were processed, shown here as separate data points with mean ± SEM. (D) Representative dot plot from ipsilateral and contralateral nerves at 10 and 14 weeks after injury, also showing the presence of a large unknown population (CD45+/CD11b−/βTCR−).

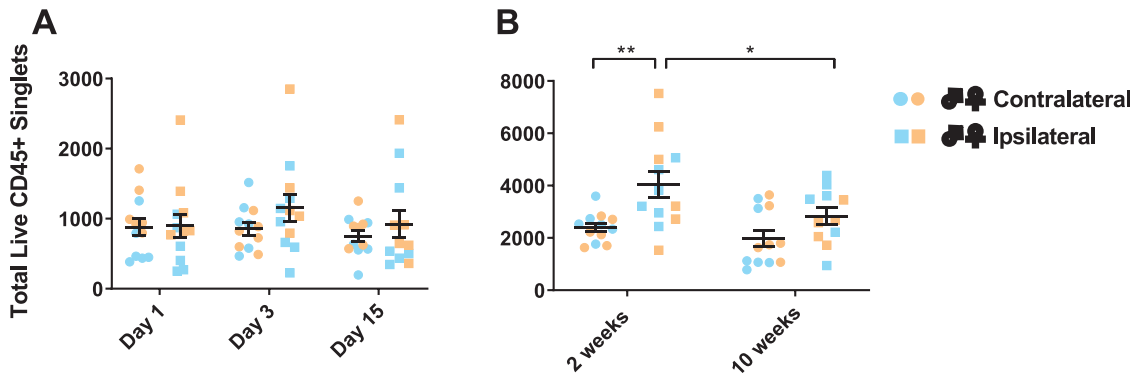

Figure 4. Total CD45+ immune cell counts in DRG are less variable over time and any increases do not persist in the long term. Plotted are the total number of live CD45+ singlets isolated from L3-5 DRG after partial sciatic nerve ligation at different time points. Results were obtained as part of 2 separate experimental batches (A and B), hence the differences in baseline counts. In both instances, n = 12 mice per time point were processed (6 males in blue and 6 females in orange), shown here as separate data points with mean ± SEM. DRG, dorsal root ganglia.

hypothesize that there are differences of small effect size, the reliable detection of which requires large samples (n = 12+) and experimental designs optimised for little variability. For instance, the data in **Figure 4A** were generated with our least optimised flow cytometry panel (Supplementary Table 1A, available at http://links.lww.com/PAIN/B19), which possibly obscured the differences visible in **Figures 4B and 5** obtained with a more evolved panel (Supplementary Table 1B, available at http://links.lww.com/PAIN/B19).

Of note, we detected a permanent CD45+/CD11b+/Ly6G+ positive population in DRG, even on the contralateral side, indicating that Ly6G+ might not be an ideal marker for neutrophils in this tissue (**Fig. 5**; and Supplementary Figure 9, available at http://links.lww.com/PAIN/B19).

3.3. No consistent sex differences in immune cell numbers

We previously detected sex differences in lymphocyte numbers when examining immune cells from DRG from a smaller number of mice (n = 4, male vs female) at 2 time points (day 8 vs day 28).[34] Our current, more thorough exploration failed to replicate this. We were unable to detect any consistent differences in immune cell numbers in either nerve or DRG after PSNL at any of the time points examined (**Fig. 6A**). There were several minor technical differences between our previous experiment in DRG and the series of studies reported here: our cell extraction methods became more streamlined and our panel evolved over time. However, we believe that the most parsimonious explanation for our previous observation is that a small n number coupled with high variability led to a false-positive result. Indeed, in our current series of experiments, statistically significant differences did emerge regularly in particular experimental batches, but ultimately failed to consistently replicate (**Fig. 6B**). Based on a wealth of previous literature,[27] we still think it probable that there are sex differences in adaptive immunity, but that they will require high power (ie, very large sample sizes and little variability) to detect.

3.4. RNA-seq results confirm antigen-presenting phenotype of MHCII+ population

Our flow cytometry results were complemented by transcriptional experiments. To gain a broad overview of different molecular phenotypes, we performed shallow sequencing on various myeloid cell subpopulations in nerve and DRG 1 and 10 weeks after PSNL, and also examined T cells from nerve at 10 weeks after PSNL. Samples included in the subsequent analyses were screened for sequencing quality: on average, 95% of reads fell within genes, and there was negligible ribosomal (1% on average) and no DNA contamination (Supplementary Table 2, available at http://links.lww.com/PAIN/B20, and for processed TPM values, see Supplementary Table 3, available at http://links.lww.com/PAIN/B79, and Table 3 on GEO:https://www.ncbi.nlm.nih.gov/geo/download/?acc=GSE139150&format=file&file=GSE139150%5FSupplementary%5FTable%5F3%5FTPM%5Fweek1%2Exlsx). On average, 7.8 M of high-quality, nonduplicate reads were captured. Samples were also relatively free of contaminating cell types, with the exception of DRG macrophages, which suffered from a small degree of contamination with satellite glial and neuronal transcripts (Supplementary Figure 10, available at http://links.lww.com/PAIN/B19). This should be considered when interpreting differentially expressed transcripts between nerve and DRG myeloid cells. It is also worth bearing in mind that any tissue dissociation and sorting technique will introduce some transcriptional artefacts, such as upregulation of immediate early genes.[65]

As expected, our sequencing samples at week 1 segregated by myeloid cell phenotype, although principal component analysis also indicated quite significant transcriptomic changes as a result of injury (**Fig. 7**), particularly in MHCII+ myeloid cells from sciatic nerve. Indeed, 279 transcripts were identified as significantly dysregulated in ipsilateral MHCII+ cells compared to their contralateral counterparts (*sleuth* algorithm,[49] adj. $P < 0.05$, for the full list of differentially expressed genes, see Table 5 on GEO: https://www.ncbi.nlm.nih.gov/geo/download/?acc=GSE139150&format=file&file=GSE139150%5FSupplementary%5FTable%5F5%5Fsleuth%5Fweek1%2Exlsx). To identify which of these genes are known to be functionally connected, we entered them into a protein–protein interaction database (STRING)[60] and annotated the resulting networks in Cytoscape.[60] The analysis suggested that, unsurprisingly, MHCII+ cells in injured nerve upregulate genes related to antigen presentation and lymphocyte interactions, but downregulate genes related to more canonical proinflammatory and resident macrophage functions (**Fig. 8**). Thus, we for instance found significantly increased expression of several MHCII genes (*H2-K1, H2Q7, H2-Oa, H2-Ob*) and of *Itgax*, the gene encoding for the dendritic cell marker CD11c. We validated the latter result at protein level (Supplementary Figure 11, available at http://links.lww.com/PAIN/B19), recording significantly more CD11c-expressing cells amongst the MHCII+/Ly6C− population in sciatic nerve 3 and 7 days after PSNL.

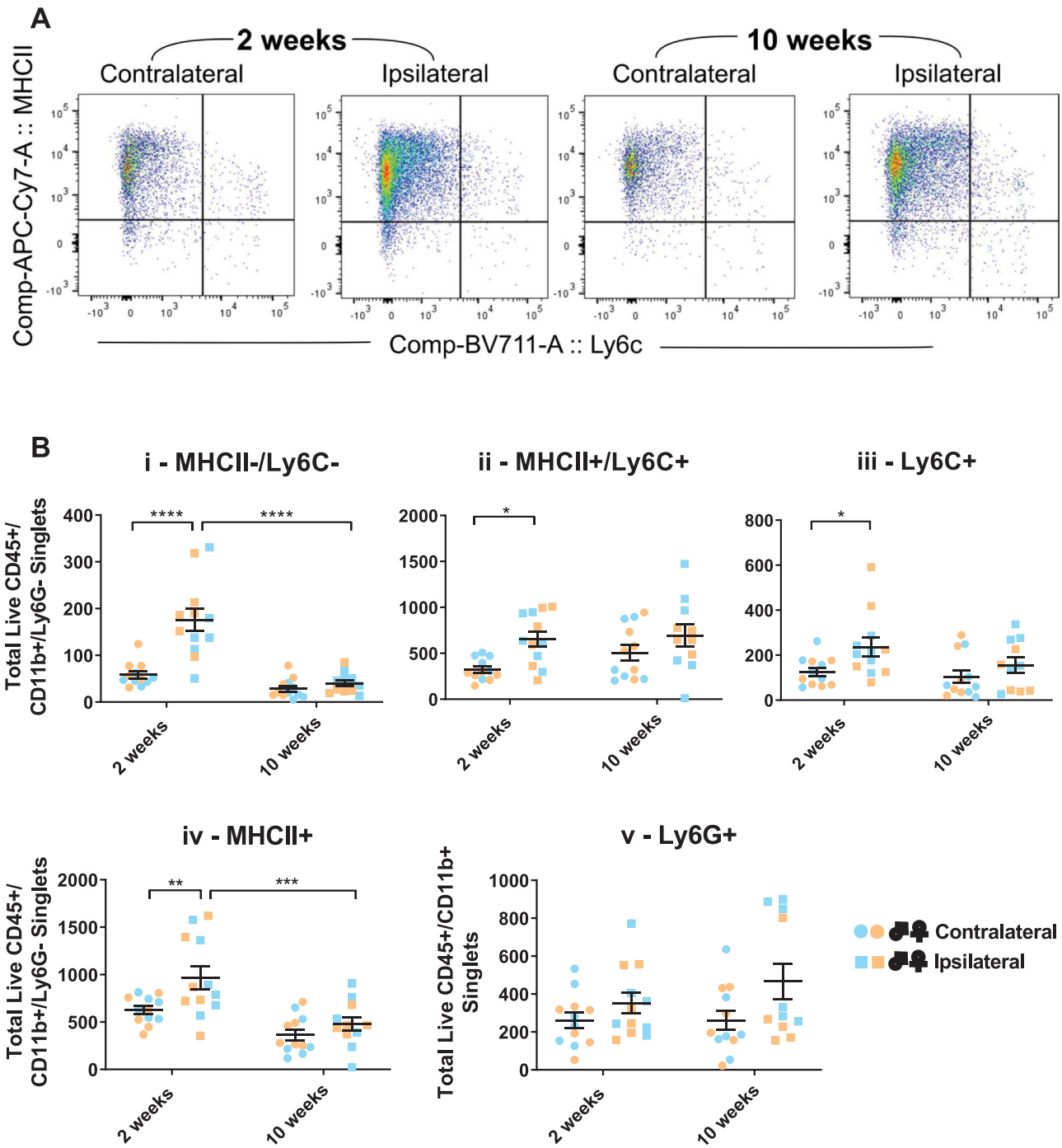

Figure 5. None of the major myeloid cell populations in the DRG remain significantly upregulated two and a half months after partial sciatic nerve ligation. (A) Flow cytometry was used to phenotype immune cell populations in DRG. Shown here are representative dot plots of myeloid subpopulations, gated on live CD45+, CD11b+, Ly6G− singlets: MHCII+ (likely resident, antigen presenting macrophages), MHCII+/Ly6C+ (likely infiltrating monocytes differentiating into resident populations), Ly6C+ (infiltrating monocytes), and MHCII−/Ly6C− (likely resident macrophages). (B) Quantification of the total number of live CD45+/CD11b+ singlets obtained from ipsilateral and contralateral DRG which were either negative for (i) MHCII−/Ly6C− or positive for (ii) MHCII+/Ly6C+, (iii) Ly6C+, (iv) MHCII+, or (v) Ly6G+ (neutrophils). At each time point, n = 12 mice were processed (6 males in blue and 6 females in orange), shown here as separate data points with mean ± SEM. Note that Ly6G in the DRG may not mark infiltrating neutrophils very effectively (see text). DRG, dorsal root ganglia.

3.5. Dorsal root ganglia macrophages are different from nerve macrophages

Also, in keeping with our cell count data, we found no striking main effect of *sex* at transcriptional level (https://osf.io/kqbxh/download), at least not beyond X- and Y-linked genes that are usually found associated with female and male sampling.[33] We could, however, detect clear differences in phenotype between macrophages from sciatic nerve and DRG. Thus, compared to nerve, MHCII+ myeloid cells from DRG expressed markers commonly associated with resident microglia (**Fig. 9A** and Supplementary Table 4, available at http://links.lww.com/PAIN/B82). This microglial-like phenotype is even more striking after injury, in that both MHCII+/Ly6C− and MHCII−/Ly6C− DRG macrophages significantly upregulated a host of known neurodegeneration-associated and homeostatic microglial markers[28] (**Fig. 10** and Supplementary Table 5, available at http://links.lww.com/PAIN/B83). These include *Trem2*, *Apoe, Csf1r, Fcrls,*

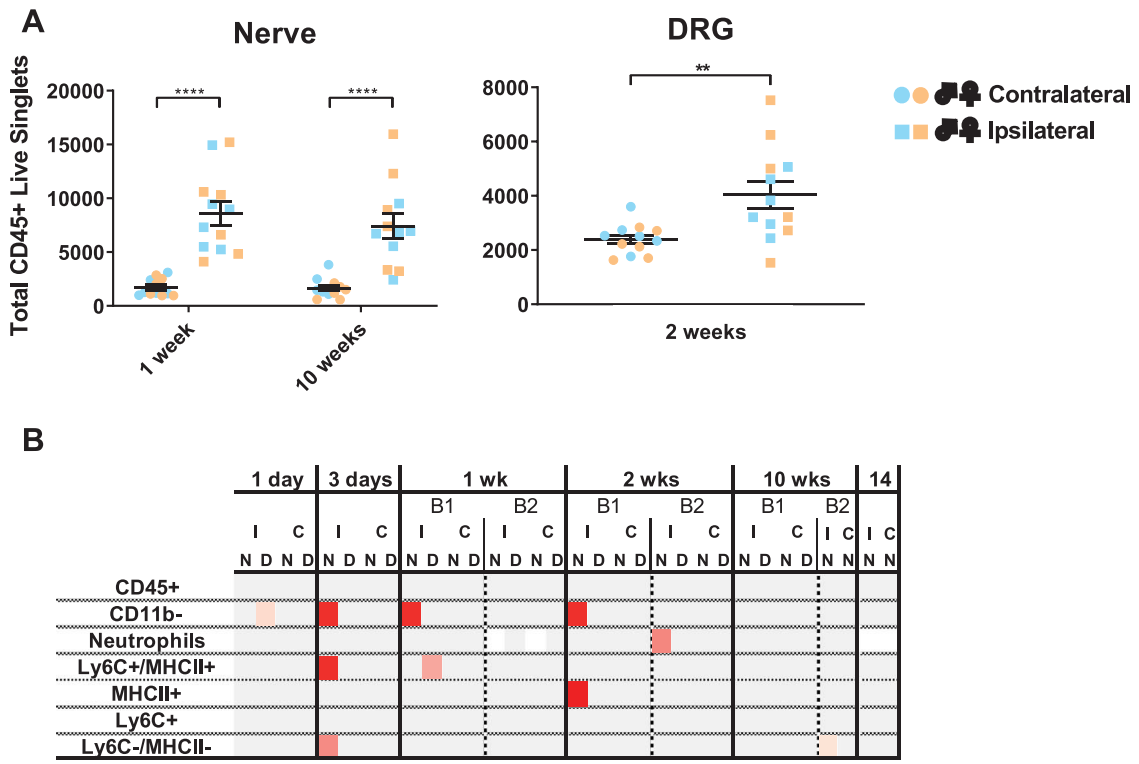

Figure 6. There are no striking sex differences in immune cell numbers in either nerve or DRG after partial sciatic nerve ligation at any of the time points. (A) Plotted are select examples of the total number of live CD45$^+$ singlets obtained from ipsilateral and contralateral nerves and DRG from male and female mice. At each time point (1 and 10 weeks after PSNL for nerve, 2 weeks after PSNL for DRG), n = 12 mice were processed (6 males in blue and 6 females in orange), shown here as separate data points with mean ± SEM. (B) Over the course of this work, immune cells were characterized at 6 different time points, with 2 batches (B) each for 1, 2, and 10 weeks after nerve injury. At each time point, we had n = 6 per male/female group (with the exception of week 14, where we had n = 11/12 per group). Plotted here is a summary of the sex differences we observed for all major populations from nerve (N) and DRG (D) in ipsilateral (I) and contralateral (C) tissue. White squares: no data collected; gray squares: no significant sex differences; graded red squares: significant sex differences with *P* values ranging from $P < 0.05$ to $P < 0.03$ and $P < 0.005$. No consistent differences emerged, suggesting that any single instance might be a false-positive event. DRG, dorsal root ganglia; PSNL, partial sciatic nerve ligation.

Tmem119, and *Olfml3.* The level of enrichment is highly unlikely to have arisen by chance, with 9x as many neurodegeneration-associated microglial genes identified in DRG as would be expected ($P < 0.0001$) and 10x as many homeostatic microglial genes ($P <$ 6.5E-12). We validated some of these results with qRT-PCR including additional biological replicates (Supplementary Figure 12, available at http://links.lww.com/PAIN/B19). *Trem2* and *Tmem119* were once more significantly dysregulated in DRG compared to nerve in this larger sample, whereas *Apoe* was not, in line with it being a more borderline result in our sequencing data. With the exception of *Abi3*, *Fscn1*, *Itgax,* and *Lgals3*, nerve MHCII+ myeloid cells showed no change in these microglial markers or significantly downregulated them with injury (in the case of *Msr1, Gas7, St3gal6, Scamp5, Csf1r, Cx3cr1, Slco2b1, Gpr34,* and *Siglech*). Compared to DRG, nerve MHCII+ myeloid cells instead expressed relatively more transcripts related to cytoskeletal organisation and wound healing (**Fig. 9B** and Supplementary Table 4, available at http://links.lww.com/PAIN/B82). Please note, however, that all these results remain to be confirmed at protein level.

The difference between nerve and ganglion may be a generic one associated with other peripheral neuron-associated macrophages. It is known that tissue-resident macrophage populations are distinct from one another, and that their development and phenotype are dependent on local environmental cues.[17,30] To investigate whether this is the case, we compared our RNA-seq to previously published data on sympathetic neuron-associated macrophages.[50] We found that genes upregulated in DRG-associated macrophages compared to nerve also seem more highly expressed in macrophages isolated from sympathetic ganglia (**Fig. 11** and Supplementary Table 4, available at http://links.lww.com/PAIN/B82). The same is true for macrophages from sciatic and sympathetic nerves, both of which resemble adipose tissue macrophages derived from subcutaneous and visceral fat.

3.6. Transcriptional changes 10 weeks after injury are different from 2 weeks, but do not yet point towards resolution of inflammation

Ten weeks after PSNL, MHCII+ myeloid cells in sciatic nerve overexpress a different set of genes in response to nerve injury compared to week 1 (**Fig. 12A** and Supplementary Table 6, available at http://links.lww.com/PAIN/B84). The lists of significantly upregulated genes at the 2 time points (110 in week 10 vs 186 in week 1) only have 4 genes in common—this is not a statistically reliable overlap and could easily arise by chance. Considering the most reliably dysregulated genes at week 10 (FC > 3), they seem to comprise transcripts relating to general myeloid cell activation, including *Ctss*, *Lgals3* (galectin-3), *Apoe*, *Fabp5*, *Itgb2*, and *Mcemp1*, and genes related to vesicle-mediated transport. A large number of transcripts seem to be related to p53 signalling (*Trp53*), which could point towards cells initiating apoptosis, entering cell cycle, or driving chronic inflammatory processes—all functions in which p53 has been implicated.[12] Related to this may be the observed changes in genes involved in the mitochondrial protein complex, some of which control the permeability of mitochondrial membranes during apoptosis (*Slc25a4, Acaa2,* and *Bloc1s2* [not in

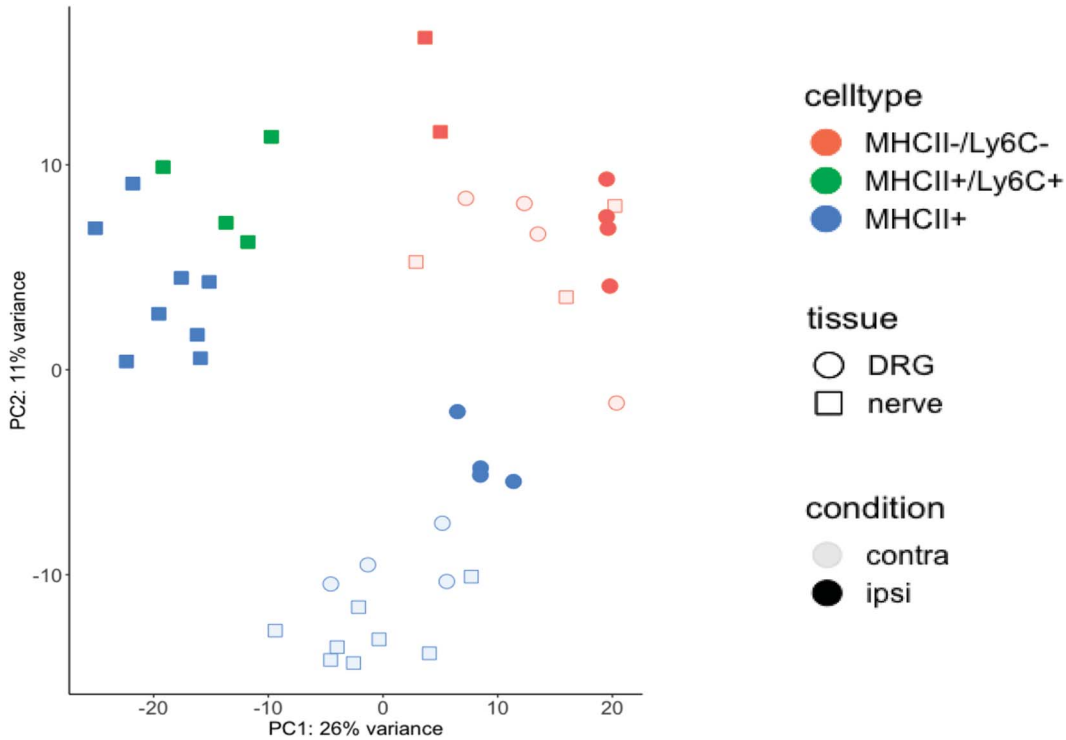

Figure 7. Principle component analysis (PCA) of FAC-sorted immune cells show they cluster by cell type, as expected, but also by injury state—suggesting significant transcriptomic changes. Principle component analysis of all samples extracted and sequenced 1 week after PSNL. The 3 main visible clusters are: (1) ipsilateral MHCII+ populations from nerve together MHCII+/Ly6C+ populations, which are only present in an injury state; (2) MHCII+/Ly6C− resident populations; and (3) MHCII+ contralateral nerve and ipsilateral and contralateral DRG populations. DRG, dorsal root ganglia; PSNL, partial sciatic nerve ligation.

network graph, but significantly dysregulated—see Supplementary Table 6]).

Conspicuously absent in the transcriptional signatures we observed were clear time-dependent changes in genes related to the resolution of inflammation (**Fig. 12B**). Receptors for specialised proresolving mediators and known markers for wound healing, resolution of inflammation, and macrophage homeostasis were regulated in similar fashion in MHCII+ myeloid cells from ipsilateral nerve—whether they were harvested 1 or 10 weeks after injury. For instance, *Arg1* and *IL10* were not expressed at either time point, *Mrc1*/CD206 was downregulated at both, and *Socs2* and *Ccl22* upregulated at both. Similarly, proinflammatory markers *Il1b* and *Ccl5* remained high over the 2 1/2 months.

With the later phases of inflammation in mind, we also examined the T-cell signature at week 10. However, the data provided more questions than answers. There were very few statistically significant changes in T cells from ipsilateral nerve vs contralateral nerve (Supplementary Table 6, available at http://links.lww.com/PAIN/B84)—possibly because our broad sorting strategy on any βTCR-positive cell introduced noise due to T-cell subtypes. For instance, it is clearly apparent that one of the ipsilateral samples did contain more CD8a transcript than the others, which were mostly CD4-positive and CD8a-negative (Supplementary Figure 10, available at http://links.lww.com/PAIN/B19).

It needs to be noted that some of our failure to observe transcriptional changes over time may have been due to lack of sensitivity. Results from the power simulation package *powsimR* indicate that the high dispersion in our week 10 MHCII+ or T-cell samples may have meant that we were only powered to detect very large effect sizes (logFC $>$ 1.4) at the n numbers we had (Supplementary Figure 13A, available at http://links.lww.com/PAIN/B19). By contrast, our MHCII nerve comparisons at week 1 were probably more adequately powered because our dispersion rates and n numbers should allow for detection of logFC $>$ 1 around 80% of the time, depending on expression level (TPM $>$ 10). False-positive rates should have been reasonable (below 5%) for all comparisons at all time points for genes expressed at TPM $>$ 10 (Supplementary Figure 13B, available at http://links.lww.com/PAIN/B19).

3.7. A dedicated web browser to examine neuroimmune interactions in the periphery

Finally, to integrate the large amount of data we generated with previously published data in an easily accessible fashion, we created a dedicated webpage to browse Neuroimmune Interactions in the Periphery (http://rna-seq-browser.herokuapp.com/). We reanalysed our own data, as well as previously published data on relevant cell types that one might want to consider when examining the expression level of one's favourite gene in peripheral neuroimmune interactions, particularly after nerve injury. Specifically, we included magnetically sorted sensory neurons and FAC-sorted satellite glial cells before and after nerve injury (GSE120284),[24] Schwann cells sorted after sciatic nerve transection (GSE103039),[10] macrophages after sciatic nerve transection (GSE106488),[61] CCR2+Cx3cr1+ macrophages after sciatic nerve crush (GSE106927),[59] and naive macrophages associated with sympathetic nerve and ganglia in adipose tissue (GSE103847).[50] To improve interstudy comparisons, we realigned our RNA-seq results using BioJupies,[62] to ensure all datasets were processed with the same *kallisto* settings. Our webpage provides a quick overview of expression patterns across murine cell types, as well as a detailed representation of all individual biological replicates

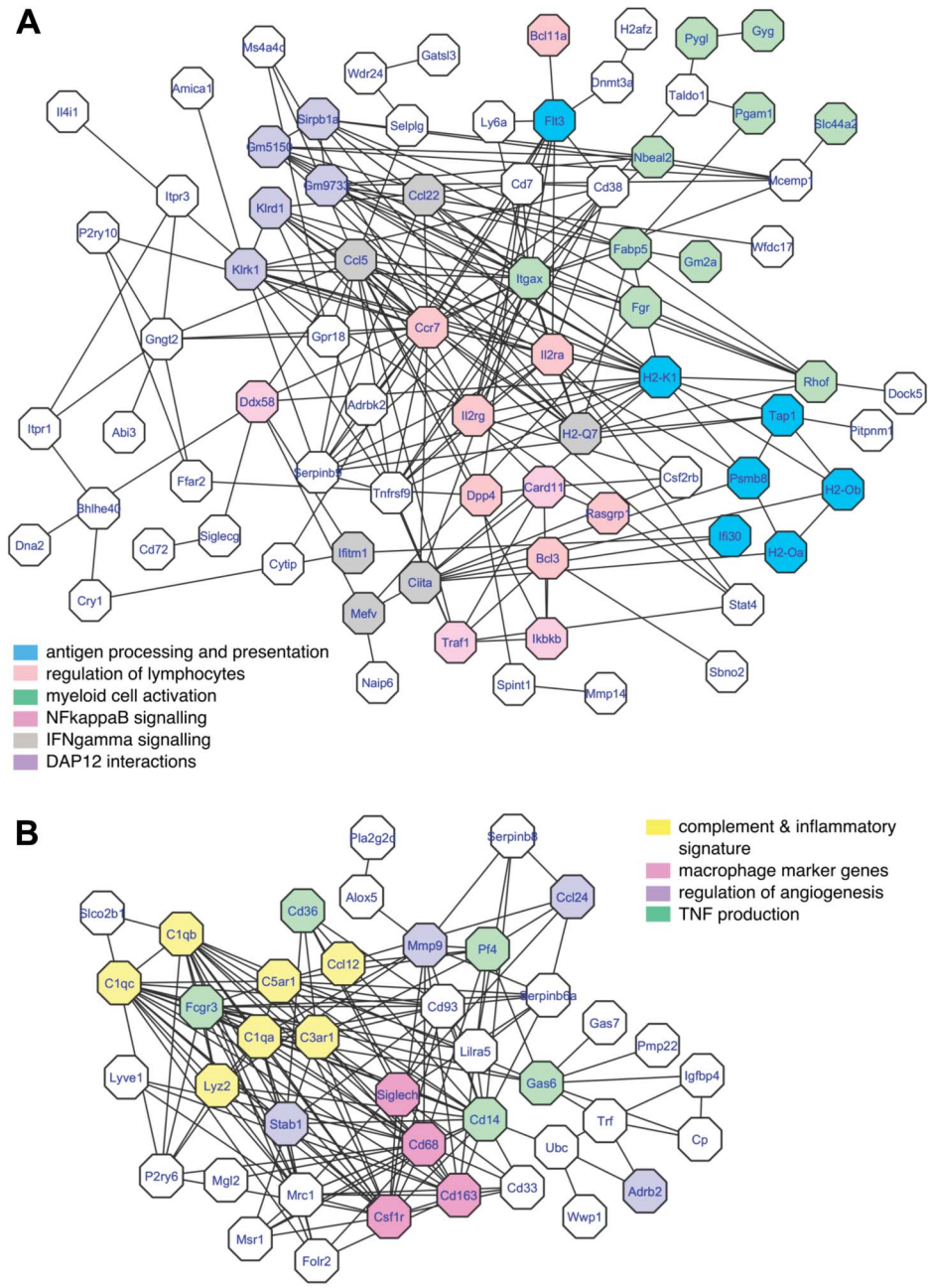

Figure 8. At 1-week after PSNL, MHCII+ myeloid cells from sciatic nerve upregulate functions relating to interactions with other immune cells, in favour of more generic proinflammatory and homeostatic activities. (A) STRING network analysis reveals that 77 of 186 genes upregulated in ipsilateral MHCII+/Ly6C− macrophages at adj. $P < 0.05$ are likely to be functionally connected with overrepresented processes including antigen presentation, regulation of lymphocytes, and myeloid cell activation. (B) Conversely, 41 of 93 significantly downregulated genes formed a network that includes transcripts relating to proinflammatory function (tumor necrosis factor, complements), regulation of angiogenesis, and canonical macrophage markers, like CD163 typically found in resident macrophages. For full differential expression tables, see Table 5 under GEO accession GSE139150: https://www.ncbi.nlm.nih.gov/geo/download/?acc=GSE139150&format=file&file=GSE139150%5FSupplementary%5FTable%5F5%5Fsleuth%5Fweek1%2Exlsx. GEO, Gene Expression Omnibus; PSNL, partial sciatic nerve ligation.

within each batch-controlled experiment. Graphs and data can be easily exported.

This web-resource can be used to confirm results reported here, eg., upregulation of CD11c (*Itgax*) in nerve macrophages can also be observed after transection (GSE106488)[61] and crush (GSE106927).[59] Or, in another example, proinflammatory cytokines such as interleukin 1 beta and tumor necrosis factor can be observed after injury in all 3 nerve macrophage data sets. In addition to validation, the website can also be used for hypothesis-generating work, as illustrated by the following 2 use-cases:

(1) A simple search for *IL10* reveals that although it is not expressed in our nerve macrophage subsets after PSNL (as shown in **Fig. 12B**), it is clearly present in 2 independent data sets examining its expression level in nerve macrophages after sciatic nerve transection and crush (**Fig. 13**). The latter 2 are models of nerve regeneration rather than permanent damage and neuropathy. Indeed, *IL10* knockout in mice has previously

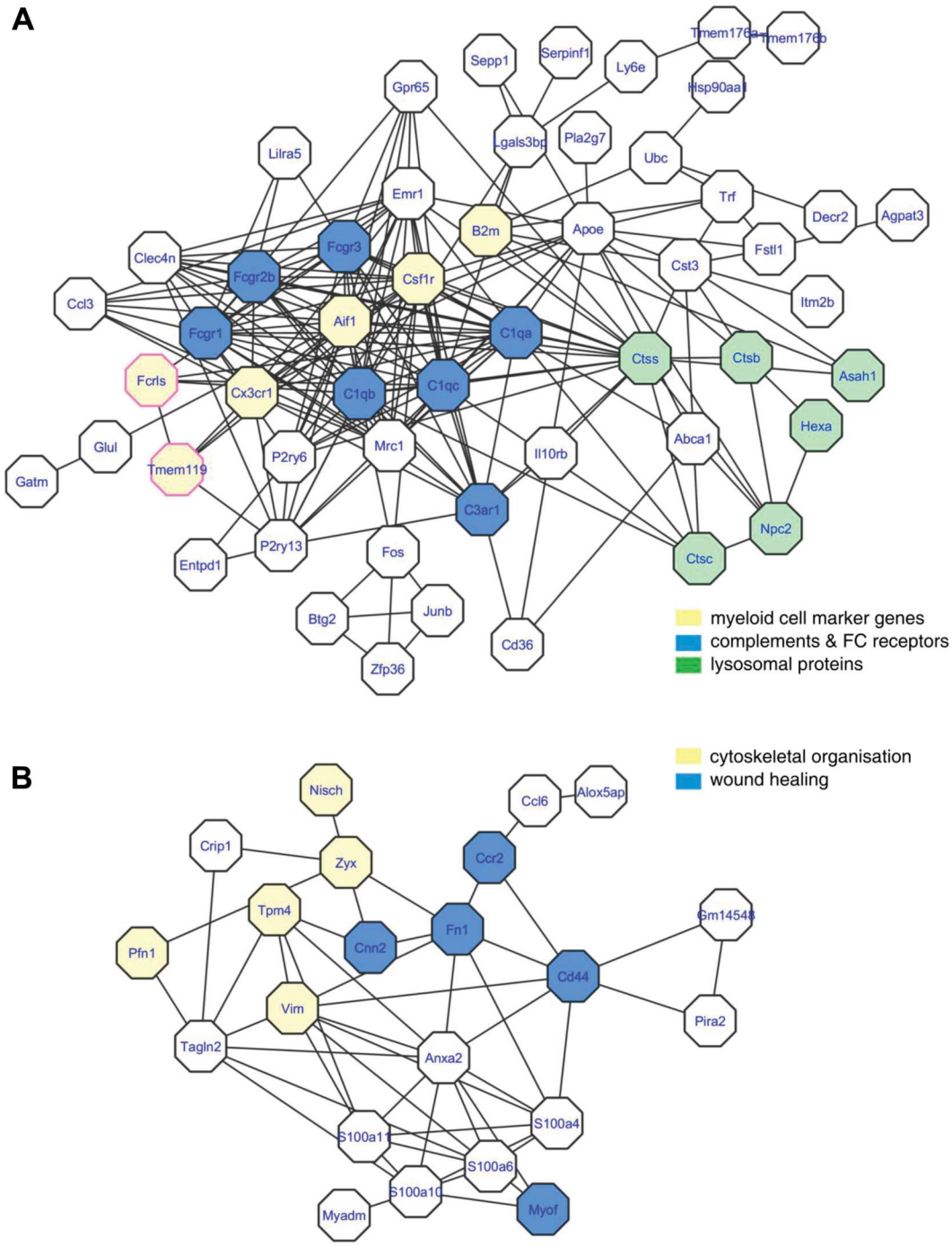

Figure 9. MHCII+ myeloid cells from DRG are different to those from sciatic nerve. (A) Genes upregulated at adj. $P < 0.05$ in MHCII+/Ly6C− macrophages from DRG vs nerve were fed into a STRING network analysis. Functional connections were found between 53 (out of a total of 93). Note the presence of canonical microglial marker genes Fcrls and Tmem119. (B) By contrast, genes upregulated in macrophages from nerve rather than DRG formed a very different functional network (22 out of 38) with processes more related to cytoskeletal organisation and wound healing. Note the presence of *Anax2* and several *S100* genes also found at high levels in adipose tissue macrophages (see Fig. 11 & Discussion). See sleuth tab in Supplementary Table 4, http://links.lww.com/PAIN/B82 for differential expression. DRG, dorsal root ganglia.

been shown to slow down the speed of resolution and nerve repair after sciatic nerve crush.[57] Moreover, IL-10—if supplemented in models of inflammatory pain—has been shown to be analgesic.[15] Our data indicate that absence of IL-10 may be one of the factors that hamper successful resolution of inflammation also in neuropathic pain.

(2) Looking at expression of the proenkephalin gene (*Penk*), we noticed that it seems to increase over time in macrophages after sciatic nerve transection (**Fig. 14A**), whereas it is once more absent in our model of sciatic nerve ligation. We reasoned that maybe *Penk* is specifically upregulated in regenerative states, with macrophages primed to be more wound-healing and less proinflammatory. To test this, we treated murine bone-marrow derived macrophages with mediators to mimic either a proinflammatory (IFNγ or LPS) or wound-healing (IL-4) activation state. We did this alone or in

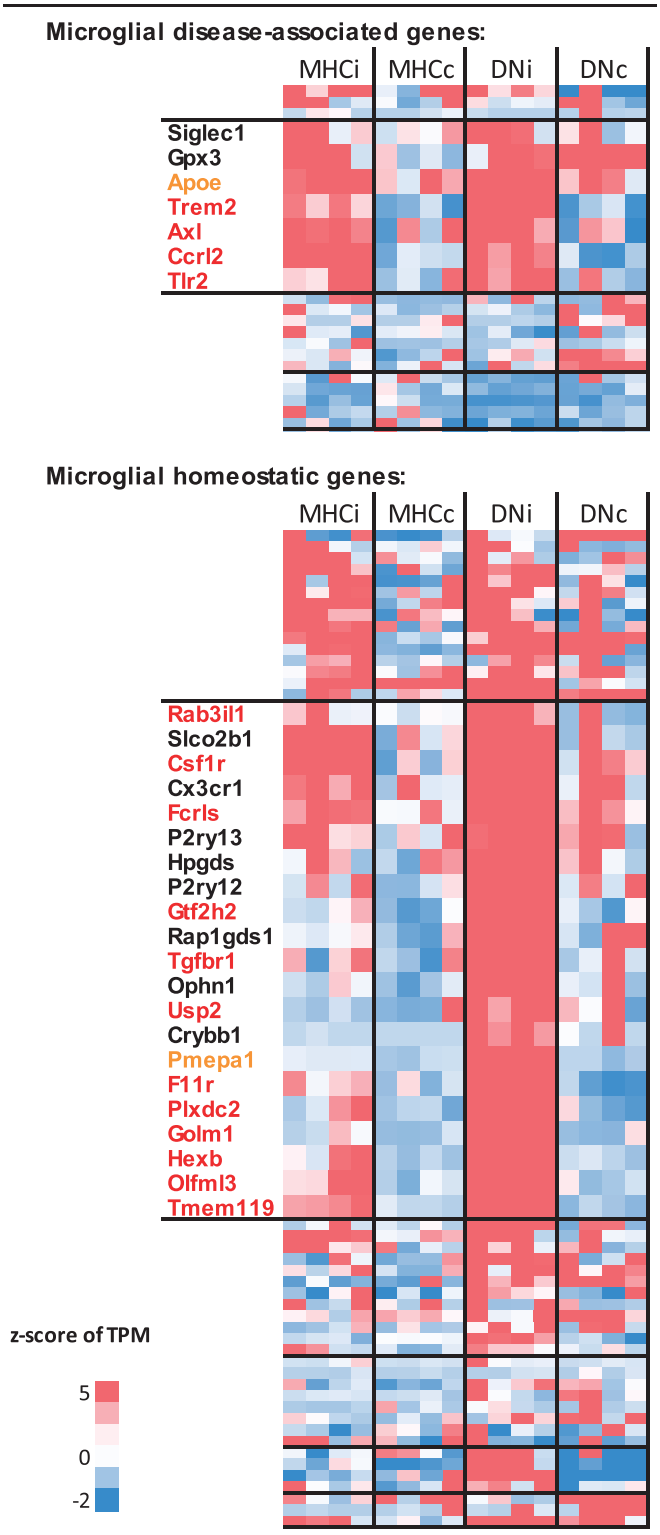

Figure 10. Macrophages in injured DRG upregulate genes associated with microglia in homeostasis and disease. Two clustergrams were generated for a list of microglial genes previously shown to be associated with disease vs homeostasis.[28] This hierarchical clustering of DRG macrophage TPM values revealed blocks of upregulated genes, particularly in the MHCII−/Ly6− resident population. Genes highlighted in red were significantly upregulated in ipsilateral macrophages at $q < 0.1$; genes highlighted in orange at $q < 0.152$. For graphing, values were converted into z space. See Supplementary Table 5, http://links.lww.com/PAIN/B83 for raw data. DRG, dorsal root ganglia; DNi, ipsilateral MHCII−/Ly6C− DRG macrophages; DNc, contralateral MHCII−/Ly6C− DRG macrophages; MHCi, ipsilateral MHCII+/Ly6C− DRG macrophages; MHCc, contralateral MHCII+/Ly6C− DRG macrophages.

combination with a neurotransmitter (calcitonin gene-related peptide, CGRP). CRGP is known to be one of the main substances by which sensory neurons communicate with immune cells.[38] We can therefore use it to mimic neuro-immune cross-talk during different macrophage activation states. *Penk* mRNA was upregulated when the macrophages were treated with IL-4, or IL-4 and CGRP. This suggests that wound healing-like macrophages, in combination with synergistic signalling from neurons, release proenkephalins (**Fig. 14B**), whereas macrophages with a more proinflammatory-like phenotype do not.

4. Discussion

Immunologists acknowledge that even "clearly defining inflammation presents a challenge."[43] Here, we attempted to move closer toward defining inflammation in a model of traumatic nerve injury. Specifically, we reveal the complexity of the immune responses at a cellular and molecular level in both nerve and DRG. We provide evidence to suggest that macrophage subpopulations in nerve and DRG are distinct entities. Sensory nerve macrophages resemble previously published transcriptional signatures of resident macrophages in adipose tissue,[50] whereas DRG macrophages resemble sympathetic ganglion macrophages[50] and resident microglia.[28] We demonstrate—in previously unprecedented detail—that resolution of inflammation after nerve injury remains elusive, even after a period of three and a half months. Finally, we identified surprisingly few consistent sex differences, neither at cellular level nor at transcriptional level.

4.1. Cellular heterogeneity of dorsal root ganglia and nerve macrophages

Our flow cytometry data show that there are 2 distinct CD11b+/Ly6G− myeloid subpopulations in nerve and DRG during homeostasis: MHCII+ and MHCII−/Ly6C−, likely equivalent to Cx3cr1+ resident populations described elsewhere.[68] After nerve injury, these are joined by Ly6C+ cells, likely infiltrating monocytes, and MHCII+/Ly6C+ double-positive cells. Our transcriptomic data confirm that MHCII+ cells are antigen-presenting and interact with lymphocytes. Without lineage tracing, it remains unclear whether we are observing antigen-presenting macrophages[41] or dendritic cells—a subtle distinction that some have anyway claimed to be moot.[23] We can, however, state that the presence of CD45ra receptor transcript (*Ptprc*), together with CD11b, makes them unlikely to be blood-derived dendritic cells, at least as defined in a consensus paper on nomenclature in 2010.[73]

Our results further suggest that, at least quantitatively, MHCII+ and MHCII−/Ly6C− macrophages are different in nerve and DRG and react differently after injury. As shown previously using immunohistochemistry,[26] we found less long-lasting proliferation/infiltration of immune cells in DRG than in nerve. Moreover, DRG macrophages resemble sympathetic ganglion macrophages and express resident myeloid cell markers, such as *Tmem119* and *Fcrls*, more prominently than nerve macrophages. Conversely, the transcriptome of nerve macrophages is much more similar to that of sympathetic nerve and adipose tissue macrophages. All 3 cell types, for instance, show relatively more mRNA expression of annexin-2 (*Anxa2*) and its interacting calcium-related adapter proteins (*S100a4, S100a6, S100a10,* and *S100a11*).[32] Annexin-S100 complexes have been implicated in various cellular functions including endocytosis, cell–cell interactions, and regulation of lipids. They have also been shown to be modulated by knockout of

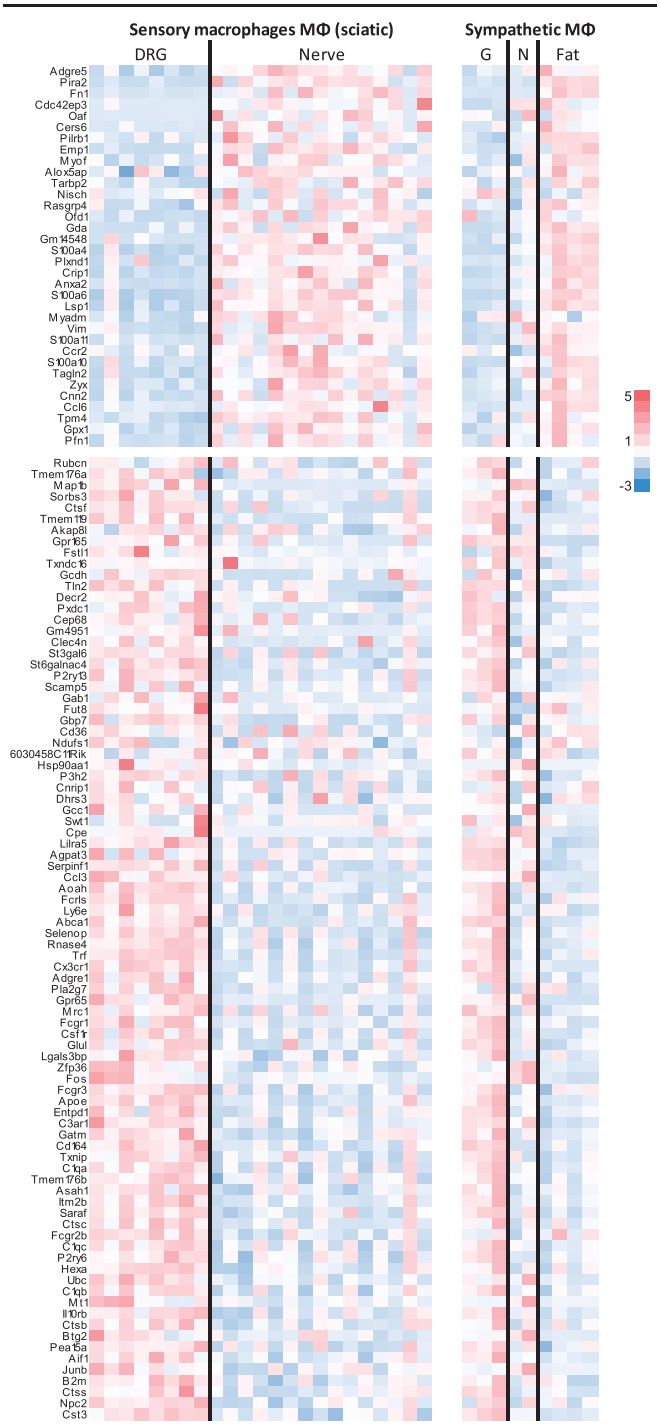

Figure 11. Macrophages from DRG resemble those from sympathetic ganglia, whereas macrophages from sciatic nerve resemble those derived from sympathetic nerve and adipose tissue. Left: Heatmap of genes significantly upregulated (top) and downregulated (bottom) in MHCII+/Ly6C− nerve vs DRG macrophages ($q < 0.05$). Plotted are TPM values for individual biological replicates, converted into z-scores per gene row. Right: RPKM values for the same list of genes obtained from GSE103847[50] (again converted into z-scores). MΦ: macrophages. DRG: dorsal root ganglia-derived macrophages. See Supplementary Table 4, http://links.lww.com/PAIN/B82 for raw data. G, macrophages derived from sympathetic ganglia; Fat, macrophages derived from subcutaneous and visceral fat; Nerve, sciatic nerve derived macrophages; N, macrophages derived from sympathetic nerve fibres of inguinal fat.

the prostaglandin COX-2,[3] the primary target of nonsteroidal anti-inflammatory painkillers. With our current set of data, it is impossible to tell whether this similarity is due to nerve and adipose tissue macrophages sharing the same lineage or whether it is merely difficult to isolate macrophages from nerve without contaminating them with those from fat.

After injury, an especially striking difference is the upregulation of neurodegeneration-associated microglial transcripts, namely *Trem2*, *Axl*, *Ccrl2,* and *Tlr2*, in MHCII+ DRG, but not nerve macrophages. The same genes are even more starkly dysregulated in MHCII−/Ly6C− populations—very clearly so in DRG, and possibly also in nerve, although the picture is less clear due to the smaller n numbers that were available for sequencing. *Trem2* has been linked to the detection of phosphatidylserine, a membrane-associated lipid that becomes exposed on apoptotic or damaged neurons.[69] Evidence suggests that this detection then "tags" the associated cell for microglial phagocytosis.[28] Our results indicate that this is not a microglial-specific process, as is often implied,[28,70] even in neuroscientific reviews that discuss its presence in macrophages.[64] This is further supported by a very recent report, which convincingly argues that high levels of *Trem2* in macrophages is a common feature of pathologies that involve lipid abnormalities because it has been reported in macrophage subpopulations of atherosclerotic aortas[11] and of liver and visceral adipose tissue in the context of obesity.[25]

Our data are also in line with a recent article confirming that naive Cx3cr1+ resident macrophages in DRG and nerve (likely equivalent to our MHCII−/Ly6C− populations) are transcriptionally distinct, but express similar mRNAs to those found in resident microglia.[68] Moreover, work from the Basbaum lab provides a functional equivalent to the expression differences we report, with evidence that ablation of DRG, but not nerve macrophages, reduces pain-like behaviour in mice after spared nerve injury.[72]

4.2. Long-lasting inflammation after nerve injury

Beyond phenotypic identity, the kinetics of the inflammatory response we observed is in keeping with what has previously been reported in the literature.[52] The time-course of neutrophil infiltration into rat nerves was previously characterised using immunohistochemistry.[47] Equivalent to our findings, the authors reported the peak of neutrophil infiltration 24 hours after PSNL, with fewer, but still noticeably elevated numbers reported 7 days after PSNL.

Similarly, there have been prior reports of persistent immune cell responses in nerve and DRG after injury, although studies beyond one month are very scarce. To the best of our knowledge, we are only aware of one series of pioneering articles by Hu & McLachlan, who examined macrophage markers in rat. They reported increased numbers of MHCII+ macrophages and T cells in sciatic nerve and DRG 10 and 11 weeks after L5 spinal nerve transection and ligation[20–22]—a result that we have now been able to replicate in nerve and extend to 14 weeks after sciatic nerve ligation. Impressively, with the help of just 3 immunohistochemical markers and careful examination of cell morphology, the group already posited the existence of 4 distinct macrophage populations in DRG[22]: CD68+/CD163+ resident macrophages, likely equivalent to our MHCII−/Ly6C− population; MHCII+ monocytes invading from blood, likely our MHCII+/Ly6C+ population; CD68+/MHCII+ cells, likely our MHCII+ population; and $CD68^+$ invading monocytes, likely our Ly6C+ population.

Although this information has been available in the literature, and immune cells are generally acknowledged to play a key role in neuropathic pain states,[4,36,55] the prevailing narrative in the pain field is still one that segregates pain into inflammatory vs neuropathic.[13,39,51,54,71] It is a clinically useful distinction because

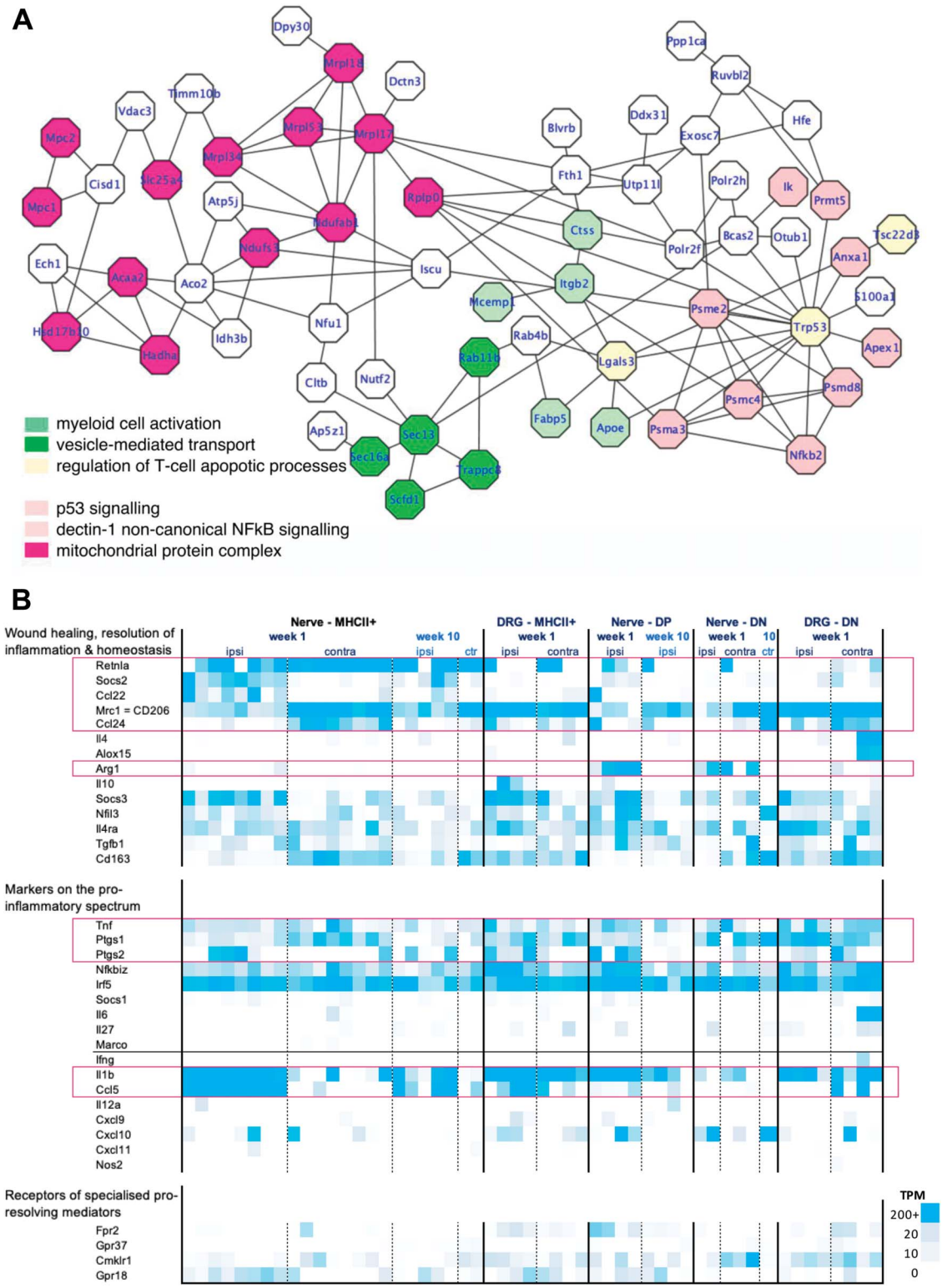

Figure 12. At 2 1/2 months after PSNL, the most prominently upregulated genes in nerve MHCII+ myeloid cells differ from those identified at week 1—but still do not include transcripts related to resolution of inflammation. (A) STRING network analysis reveals that 63 of 110 genes upregulated in ipsilateral MHCII+/Ly6C− macrophages at adj. $P < 0.05$ and FC > 3 are likely to be functionally connected with overrepresented processes including myeloid cell activation, vesicle-mediated transport, and regulation of T-cell apoptosis. See Supplementary Table 6, http://links.lww.com/PAIN/B84, for full differential expression tables. (B) Heat map of genes that the expression of which one might expect to see varied with resolution of inflammation. Plotted are TPM expression values from low (white, TPM = 0) to high (darkest blue). MHC+: MHCII+/Ly6C− macrophages. DN: MHCII−/Ly6C− macrophages. See https://osf.io/uy9pm/download for raw data. DP, MHCII+/Ly6C+ macrophages; TPM, transcripts per million; PSNL, partial sciatic nerve ligation.

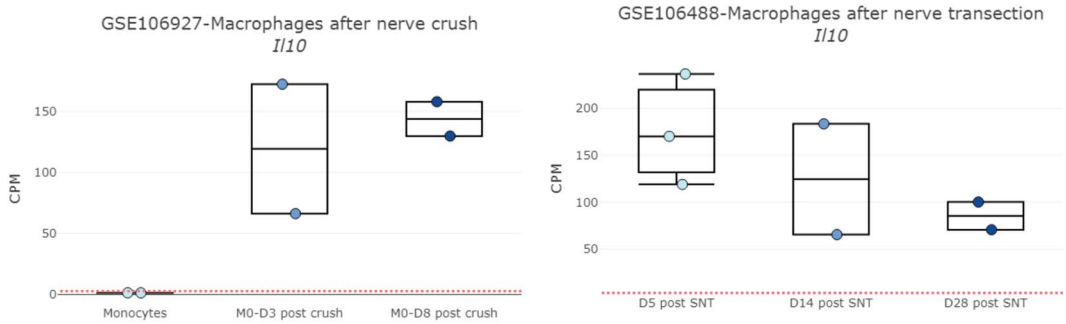

Figure 13. Graphs downloaded with one click from our novel web-resource, which allows browsing of cell-type-specific RNA-seq data relevant for peripheral neuroimmune interactions. The cytokine IL10, which has a known role in resolution of inflammation, is clearly expressed in macrophages collected from sciatic nerve after regenerating nerve lesions. Data are derived from 2 independent studies (GEO identifiers GSE106927 and GSE106488) and are plotted as counts per million (CPM), ie, raw counts normalised by the total read count per sample. The dotted red line represents a threshold value below which gene expression is likely to fall within the noise range. Each dot is an independent biological replicate. GEO, Gene Expression Omnibus.

neuropathic pain patients do not respond to nonsteroidal anti-inflammatory medications. However, we would argue that from a preclinical perspective, this dichotomy evokes dangerously misleading ideas that imply that neuropathic pain states involve "less" inflammation or immune cell activation within the affected tissues. This is emphatically not the case: our data demonstrate that one of the most commonly used animal models of traumatic nerve injury is accompanied by a significant and persistent inflammatory response, which is unresolved for 3 1/2 months—for as long as we were permitted to measure it by our ethical review board.

4.3. Limitations

With the exception of MHCII nerve samples at week 1, our RNA-seq data were only powered to detect very striking differences, due to a combination of shallow read depth and high variance between samples. Moreover, transcripts with TPM <10 are unlikely to have been adequately represented, both in terms of their expression levels and their variation with injury. It is important to bear this in mind when examining our data—or indeed those of others. Due to cost implications, many published RNA sequencing results will not be adequately powered to detect changes in more lowly expressed genes. Our simulation data indicate that given the high dispersion that is likely be present in bulk transcriptional data of small numbers of sorted immune cells, you would require at least an n = 16 to be comfortably powered to detect an effect size of logFC > 1 at all expression levels (Supplementary Figure 13, available at http://links.lww.com/PAIN/B19).

Although we are confident that there are transcriptional differences between nerve and DRG, it is unclear how this will translate to protein level. Studies comparing these 2 tissues with antibodies are outstanding and necessary.

Regarding sex differences, we would like to stress that the absence of consistent sex differences in our flow and RNA-seq data does not mean that they are not present at lower effect sizes that we were not powered to detect. We would also like to emphatically endorse the importance of sex and gender considerations when studying neuroimmune interactions—especially because they are known to play prominent roles in the perception of pain, chronic pain conditions, and immune system function.[6,18,19,27,40] Instead, we see our results as a timely

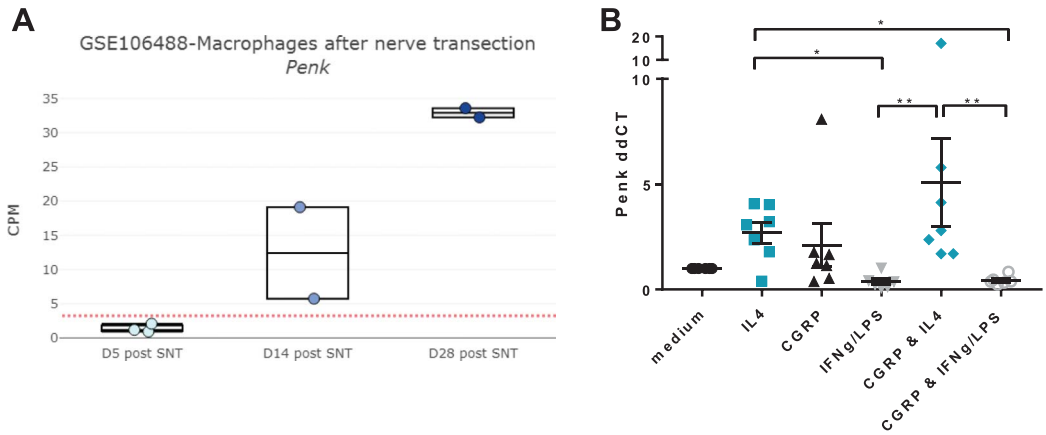

Figure 14. Our web-resource allows formulating and testing of novel hypotheses. (A) Macrophages isolated from regenerative sciatic nerve after transection seem to progressively increase expression of proenkephalin (*Penk*)—data published under GEO identifier GSE106488 and plotted on our web-resource at counts per million (CPM), ie, raw counts normalised by the total read count per sample. The dotted red line represents a threshold value below which gene expression is likely to fall within the noise range. Each dot is an independent biological replicate. (B) qRT-PCR for *Penk* conducted on bone marrow-derived macrophages treated with IL-4 or the proinflammatory cytokines IFNγ or LPS with or without the neurotransmitter CGRP. IL-4 treatment alone and IL-4 in combination with CGRP significantly upregulated *Penk* expression: Kruskal–Wallis ANOVA $X^2(6) = 25.77$, $P = 0.0001$, with Dunn multiple comparisons: $^*P < 0.03$, $^{**}P < 0.005$. Data points represent values obtained from n = 6 to 7 independent BMDM culture experiments. Mean ± SEM are also plotted. ANOVA, analysis of variance; BMDM, bone marrow-derived macrophage; GEO, Gene Expression Omnibus.

reminder of the ease with which a single, conventionally sized experiment (n = 4 biological replicates) can yield false-positive findings when dealing with variable in vivo samples. It is a trap into which we ourselves seem to have fallen,[34] and which is especially tempting when results align with what is considered to be the most probable hypothesis, namely that there are sex differences in adaptive immunity.

In conclusion, we used a model of traumatic neuropathic pain to study peripheral neuroimmune interactions in the context of injury. Our findings point towards a very complex and long-lasting inflammatory response. To help other researchers in this area, we are providing an easy-to-use plug-and-play website that allows mining of relevant cell-type-specific RNA-sequencing data sets in naive and nerve injury conditions.

Conflict of interest statement

The authors have no conflicts of interest to declare.

Acknowledgements

This work has received funding from an MRC New Investigator Grant (MR/P010814/01) and the Innovative Medicines Initiative 2 Joint Undertaking under Grant Agreement no. 116072. This Joint Undertaking receives the support from the European Union's Horizon 2020 research and innovation. The authors thank the Oxford Genomics Centre at the Wellcome Centre for Human Genetics (funded by Wellcome Trust grant reference 203141/Z/16/Z) for the generation and initial processing of the sequencing data. The authors acknowledge financial support from the Department of Health via the National Institute for Health Research (NIHR) comprehensive Biomedical Research Centre award to Guy's & St Thomas'NHS Foundation Trust in partnership with King's College London and King's College Hospital NHS Foundation Trust.

Appendix A. Supplemental digital content

Supplemental digital content associated with this article can be found online at http://links.lww.com/PAIN/B19, http://links.lww.com/PAIN/B20, http://links.lww.com/PAIN/B79, http://links.lww.com/PAIN/B82, http://links.lww.com/PAIN/B83, http://links.lww.com/PAIN/B84, and https://osf.io/3q9ve/.

Supplemental video content

A video abstract associated with this article can be found at http://links.lww.com/PAIN/B85.

Article history:
Received 28 November 2019
Received in revised form 14 April 2020
Accepted 16 April 2020
Available online 24 June 2020

References

[1] A current view on inflammation. Nat Immunol 2017;18:825.
[2] Afonina IS, Zhong Z, Karin M, Beyaert R. Limiting inflammation—the negative regulation of NF-κB and the NLRP3 inflammasome. Nat Immunol 2017;18:861.
[3] Amadio P, Tarantino E, Sandrini L, Tremoli E, Barbieri S. Prostaglandin-endoperoxide synthase-2 deletion affects the natural trafficking of Annexin A2 in monocytes and favours venous thrombosis in mice. Thromb Haemost 2017;117:1486–97.
[4] Austin PJ, Moalem-Taylor G. The neuro-immune balance in neuropathic pain: involvement of inflammatory immune cells, immune-like glial cells and cytokines. J Neuroimmunol 2010;229:26–50.
[5] Barclay J, Clark AK, Ganju P, Gentry C, Patel S, Wotherspoon G, Buxton F, Song C, Ullah J, Winter J, Fox A, Bevan S, Malcangio M. Role of the cysteine protease cathepsin S in neuropathic hyperalgesia. PAIN 2007;130:225–34.
[6] Bartley EJ, Fillingim RB. Sex differences in pain: a brief review of clinical and experimental findings. Br J Anaesth 2013;111:52–8.
[7] Bolger AM, Lohse M, Usadel B. Trimmomatic: a flexible trimmer for Illumina sequence data. Bioinformatics 2014;30:2114–20.
[8] Bray NL, Pimentel H, Melsted P, Pachter L. Near-optimal probabilistic RNA-seq quantification. Nat Biotechnol 2016;34:525–7.
[9] Breivik H, Collett B, Ventafridda V, Cohen R, Gallacher D. Survey of chronic pain in Europe: prevalence, impact on daily life, and treatment. Eur J Pain 2006;10:287–333.
[10] Clements MP, Byrne E, Camarillo Guerrero LF, Cattin AL, Zakka L, Ashraf A, Burden JJ, Khadayate S, Lloyd AC, Marguerat S, Parrinello S. The wound microenvironment reprograms Schwann cells to invasive mesenchymal-like cells to drive peripheral nerve regeneration. Neuron 2017;96:98–114.e117.
[11] Cochain C, Vafadarnejad E, Arampatzi P, Pelisek J, Winkels H, Ley K, Wolf D, Saliba AE, Zernecke A. Single-cell RNA-seq reveals the transcriptional landscape and heterogeneity of aortic macrophages in murine atherosclerosis. Circ Res 2018;122:1661–74.
[12] Cooks T, Harris CC, Oren M. Caught in the cross fire: p53 in inflammation. Carcinogenesis 2014;35:1680–90.
[13] Devor M. Neuropathic pain: pathophysiological response of nerves to injury. In: McMahon SB, Koltzenburg M, Tracey I, Turk DC, editors. Wall and Melzack's textbook of pain. Philadelphia: Elsevier, 2013. pp. 861–88.
[14] Dubový P. Wallerian degeneration and peripheral nerve conditions for both axonal regeneration and neuropathic pain induction. Ann Anat 2011;193:267–75.
[15] Eijkelkamp N, Steen-Louws C, Hartgring SA, Willemen HL, Prado J, Lafeber FP, Heijnen CJ, Hack CE, van Roon JA, Kavelaars A. IL4-10 fusion protein is a novel drug to treat persistent inflammatory pain. J Neurosci 2016;36:7353–63.
[16] Ghasemlou N, Chiu IM, Julien JP, Woolf CJ. CD11b+Ly6G−myeloid cells mediate mechanical inflammatory pain hypersensitivity. Proc Natl Acad Sci 2015;112:E6808–17.
[17] Gosselin D, Link VM, Romanoski CE, Fonseca GJ, Eichenfield DZ, Spann NJ, Stender JD, Chun HB, Garner H, Geissmann F, Glass CK. Environment drives selection and function of enhancers controlling tissue-specific macrophage identities. Cell 2014;159:1327–40.
[18] Gupta A, Mayer EA, Fling C, Labus JS, Naliboff BD, Hong JY, Kilpatrick LA. Sex-based differences in brain alterations across chronic pain conditions. J Neurosci Res 2017;95:604–16.
[19] Hashmi JA, Davis KD. Deconstructing sex differences in pain sensitivity. PAIN 2014;155:10–13.
[20] Hu P, Bembrick AL, Keay KA, McLachlan EM. Immune cell involvement in dorsal root ganglia and spinal cord after chronic constriction or transection of the rat sciatic nerve. Brain Behav Immun 2007;21:599–616.
[21] Hu P, McLachlan EM. Macrophage and lymphocyte invasion of dorsal root ganglia after peripheral nerve lesions in the rat. Neuroscience 2002;112:23–38.
[22] Hu P, McLachlan EM. Distinct functional types of macrophage in dorsal root ganglia and spinal nerves proximal to sciatic and spinal nerve transections in the rat. Exp Neurol 2003;184:590–605.
[23] Hume DA. Macrophages as APC and the dendritic cell myth. J Immunol 2008;181:5829–35.
[24] Jager SE, Pallesen LT, Richner M, Harley P, Hore Z, McMahon S, Denk F, Vaegter CB. Changes in the transcriptional fingerprint of satellite glial cells following peripheral nerve injury. Glia 2020;68:1375–95.
[25] Jaitin DA, Adlung L, Thaiss CA, Weiner A, Li B, Descamps H, Lundgren P, Bleriot C, Liu Z, Deczkowska A, Keren-Shaul H, David E, Zmora N, Eldar SM, Lubezky N, Shibolet O, Hill DA, Lazar MA, Colonna M, Ginhoux F, Shapiro H, Elinav E, Amit I. Lipid-associated macrophages control metabolic homeostasis in a trem2-dependent manner. Cell 2019;178:686–98.e614.
[26] Kim CF, Moalem-Taylor G. Detailed characterization of neuro-immune responses following neuropathic injury in mice. Brain Res 2011;1405:95–108.
[27] Klein SL, Flanagan KL. Sex differences in immune responses. Nat Rev Immunol 2016;16:626–38.
[28] Krasemann S, Madore C, Cialic R, Baufeld C, Calcagno N, El Fatimy R, Beckers L, O'Loughlin E, Xu Y, Fanek Z, Greco DJ, Smith ST, Tweet G, Humulock Z, Zrzavy T, Conde-Sanroman P, Gacias M, Weng Z, Chen H,

Tjon E, Mazaheri F, Hartmann K, Madi A, Ulrich JD, Glatzel M, Worthmann A, Heeren J, Budnik B, Lemere C, Ikezu T, Heppner FL, Litvak V, Holtzman DM, Lassmann H, Weiner HL, Ochando J, Haass C, Butovsky O. The TREM2-APOE pathway drives the transcriptional phenotype of dysfunctional microglia in neurodegenerative diseases. Immunity 2017; 47:566–81.e569.
[29] Lachmann A, Torre D, Keenan AB, Jagodnik KM, Lee HJ, Wang L, Silverstein MC, Ma'ayan A. Massive mining of publicly available RNA-seq data from human and mouse. Nat Commun 2018;9:1366.
[30] Lavin Y, Winter D, Blecher-Gonen R, David E, Keren-Shaul H, Merad M, Jung S, Amit I. Tissue-resident macrophage enhancer landscapes are shaped by the local microenvironment. Cell 2014;159:1312–26.
[31] Liu T, van Rooijen N, Tracey DJ. Depletion of macrophages reduces axonal degeneration and hyperalgesia following nerve injury. PAIN 2000; 86:25–32.
[32] Liu Y, Myrvang HK, Dekker LV. Annexin A2 complexes with S100 proteins: structure, function and pharmacological manipulation. Br J Pharmacol 2015;172(7):1664–76.
[33] Lopes DM, Denk F, McMahon SB. The molecular fingerprint of dorsal root and trigeminal ganglion neurons. Front Mol Neurosci 2017;10:304.
[34] Lopes DM, Malek N, Edye M, Jager SB, McMurray S, McMahon SB, Denk F. Sex differences in peripheral not central immune responses to pain-inducing injury. Sci Rep 2017;7:16460.
[35] Lunter G, Goodson M. Stampy: a statistical algorithm for sensitive and fast mapping of Illumina sequence reads. Genome Res 2011;21:936–9.
[36] Marchand F, Perretti M, McMahon SB. Role of the Immune system in chronic pain. Nat Rev Neurosci 2005;6:521–32.
[37] McMahon SB. NGF as a mediator of inflammatory pain. Philos Trans R Soc Lond Ser B Biol Sci 1996;351:431–40.
[38] McMahon SB, La Russa F, Bennett DL. Crosstalk between the nociceptive and immune systems in host defence and disease. Nat Rev Neurosci 2015;16:389–402.
[39] Moalem G, Tracey DJ. Immune and inflammatory mechanisms in neuropathic pain. Brain Res Rev 2006;51:240–64.
[40] Mogil JS. Sex differences in pain and pain inhibition: multiple explanations of a controversial phenomenon. Nat Rev Neurosci 2012;13:859–66.
[41] Mosser DM, Edwards JP. Exploring the full spectrum of macrophage activation. Nat Rev Immunol 2008;8:958–69.
[42] Myers RR, Heckman HM, Rodriguez M. Reduced hyperalgesia in nerve-injured WLD mice: relationship to nerve fiber phagocytosis, axonal degeneration, and regeneration in normal mice. Exp Neurol 1996;141: 94–101.
[43] Netea MG, Balkwill F, Chonchol M, Cominelli F, Donath MY, Giamarellos-Bourboulis EJ, Golenbock D, Gresnigt MS, Heneka MT, Hoffman HM, Hotchkiss R, Joosten LAB, Kastner DL, Korte M, Latz E, Libby P, Mandrup-Poulsen T, Mantovani A, Mills KHG, Nowak KL, O'Neill LA, Pickkers P, Van Der Poll T, Ridker PM, Schalkwijk J, Schwartz DA, Siegmund B, Steer CJ, Tilg H, Van Der Meer JWM, Van De Veerdonk FL, Dinarello CA. A guiding map for inflammation. Nat Immunol 2017;18: 826–31.
[44] Netea MG, Balkwill F, Chonchol M, Cominelli F, Donath MY, Giamarellos-Bourboulis EJ, Golenbock D, Gresnigt MS, Heneka MT, Hoffman HM, Hotchkiss R, Joosten LAB, Kastner DL, Korte M, Latz E, Libby P, Mandrup-Poulsen T, Mantovani A, Mills KHG, Nowak KL, O'Neill LA, Pickkers P, van der Poll T, Ridker PM, Schalkwijk J, Schwartz DA, Siegmund B, Steer CJ, Tilg H, van der Meer JWM, van de Veerdonk FL, Dinarello CA. A guiding map for inflammation. Nat Immunol 2017;18:826.
[45] Neumann S, Doubell TP, Leslie T, Woolf CJ. Inflammatory pain hypersensitivity mediated by phenotypic switch in myelinated primary sensory neurons. Nature 1996;384:360–4.
[46] Old EA, Nadkarni S, Grist J, Gentry C, Bevan S, Kim KW, Mogg AJ, Perretti M, Malcangio M. Monocytes expressing CX3CR1 orchestrate the development of vincristine-induced pain. J Clin Invest 2014;124: 2023–36.
[47] Perkins NM, Tracey DJ. Hyperalgesia due to nerve injury: role of neutrophils. Neuroscience 2000;101:745–57.
[48] Picelli S, Faridani OR, Björklund ÅK, Winberg G, Sagasser S, Sandberg R. Full-length RNA-seq from single cells using Smart-seq2. Nat Protoc 2014;9:171–81.
[49] Pimentel H, Bray NL, Puente S, Melsted P, Pachter L. Differential analysis of RNA-seq incorporating quantification uncertainty. Nat Methods 2017; 14:687–90.
[50] Pirzgalska RM, Seixas E, Seidman JS, Link VM, Sánchez NM, Mahú I, Mendes R, Gres V, Kubasova N, Morris I, Arús BA, Larabee CM, Vasques M, Tortosa F, Sousa AL, Anandan S, Tranfield E, Hahn MK, Iannacone M, Spann NJ, Glass CK, Domingos AI. Sympathetic neuron–associated macrophages contribute to obesity by importing and metabolizing norepinephrine. Nat Med 2017;23:1309.
[51] Ren K, Dubner R. Interactions between the immune and nervous systems in pain. Nat Med 2010;16:1267–76.
[52] Ristoiu V. Contribution of macrophages to peripheral neuropathic pain pathogenesis. Life Sci 2013;93:870–81.
[53] Schaible HG, Ebersberger A, Von Banchet GS. Mechanisms of pain in arthritis. Ann N Y Acad Sci 2002;966:343–54.
[54] Scholz J, Woolf CJ. Can we conquer pain? Nat Neurosci 2002;5(supp): 1062–7.
[55] Scholz J, Woolf CJ. The neuropathic pain triad: neurons, immune cells and glia. Nat Neurosci 2007;10:1361–8.
[56] Seltzer Ze, Dubner R, Shir Y. A novel behavioral model of neuropathic pain disorders produced in rats by partial sciatic nerve injury. PAIN 1990;43: 205–18.
[57] Siqueira Mietto B, Kroner A, Girolami EI, Santos-Nogueira E, Zhang J, David S. Role of IL-10 in resolution of inflammation and functional recovery after peripheral nerve injury. J Neurosci 2015;35:16431–42.
[58] Soneson C, Love MI, Robinson MD. Differential analyses for RNA-seq: transcript-level estimates improve gene-level inferences. F1000Research 2015;4:1521.
[59] Stratton JA, Holmes A, Rosin NL, Sinha S, Vohra M, Burma NE, Trang T, Midha R, Biernaskie J. Macrophages regulate Schwann cell maturation after nerve injury. Cell Rep 2018;24:2561–72.e2566.
[60] Szklarczyk D, Gable AL, Lyon D, Junge A, Wyder S, Huerta-Cepas J, Simonovic M, Doncheva NT, Morris JH, Bork P, Jensen LJ, Mering CV. STRING v11: protein–protein association networks with increased coverage, supporting functional discovery in genome-wide experimental datasets. Nucleic Acids Res 2018;47:D607–13.
[61] Tomlinson JE, Žygelytė E, Grenier JK, Edwards MG, Cheetham J. Temporal changes in macrophage phenotype after peripheral nerve injury. J Neuroinflammation 2018;15:185.
[62] Torre D, Lachmann A, Ma'ayan A. BioJupies: automated generation of interactive notebooks for RNA-seq data analysis in the cloud. Cell Syst 2018;7:556–61.e553.
[63] Treede RD, Rief W, Barke A, Aziz Q, Bennett MI, Benoliel R, Cohen M, Evers S, Finnerup NB, First MB, Giamberardino MA, Kaasa S, Korwisi B, Kosek E, Lavand'homme P, Nicholas M, Perrot S, Scholz J, Schug S, Smith BH, Svensson P, Vlaeyen JWS, Wang SJ. Chronic pain as a symptom or a disease: the IASP Classification of Chronic Pain for the International Classification of Diseases (ICD-11). PAIN 2019;160:19–27.
[64] Ulland TK, Colonna M. TREM2—a key player in microglial biology and Alzheimer disease. Nat Rev Neurol 2018;14:667–75.
[65] van den Brink SC, Sage F, Vertesy A, Spanjaard B, Peterson-Maduro J, Baron CS, Robin C, van Oudenaarden A. Single-cell sequencing reveals dissociation-induced gene expression in tissue subpopulations. Nat Methods 2017;14:935–6.
[66] Vega-Avelaira D, Geranton SM, Fitzgerald M. Differential regulation of immune responses and macrophage/neuron interactions in the dorsal root ganglion in young and adult rats following nerve injury. Mol Pain 2009;5:70.
[67] Vieth B, Ziegenhain C, Parekh S, Enard W, Hellmann I. powsimR: power analysis for bulk and single cell RNA-seq experiments. Bioinformatics 2017;33:3486–8.
[68] Wang PL, Yim AK, Kim K, Avey D, Czepielewski RS, Colonna M, Milbrandt J, Randolph GJ. Peripheral nerve resident macrophages are microglia-like cells with tissue-specific programming. bioRxiv 2019:2019. 2012.2019.883546.
[69] Wang Y, Cella M, Mallinson K, Ulrich JD, Young KL, Robinette ML, Gilfillan S, Krishnan GM, Sudhakar S, Zinselmeyer BH, Holtzman DM, Cirrito JR, Colonna M. TREM2 lipid sensing sustains the microglial response in an alzheimer's disease model. Cell 2015;160:1061–71.
[70] Yeh FL, Hansen DV, Sheng M. TREM2, microglia, and neurodegenerative diseases. Trends Mol Med 2017;23:512–33.
[71] Yezierski RP, Hansson P. Inflammatory and neuropathic pain from bench to bedside: what went wrong? J Pain 2018;19:571–88.
[72] Yu X, Liu H, Hamel KA, Morvan MG, Yu S, Leff J, Guan Z, Braz JM, Basbaum AI. Dorsal root ganglion macrophages contribute to both the initiation and persistence of neuropathic pain. Nat Commun 2020; 11:264.
[73] Ziegler-Heitbrock L, Ancuta P, Crowe S, Dalod M, Grau V, Hart DN, Leenen PJM, Liu YJ, Macpherson G, Randolph GJ, Scherberich J, Schmitz J, Shortman K, Sozzani S, Strobl H, Zembala M, Austyn JM, Lutz MB. Nomenclature of monocytes and dendritic cells in blood. Blood 2010;116:e74–80.